ACIBADEM MEHMET ALI AYDINLAR UNIVERSITY
INSTITUTE OF HEALTH SCIENCES

IDENTIFICATION OF INTERACTION PARTNERS OF β1 SUBUNIT OF Na^+/K^+-ATPASE PUMP (NKA) IN IN-VITRO HYPOXIC CARDIOMYOCYTES

BEYZA GÜRLER

M.Sc. THESIS

DEPARTMENT OF MEDICAL BIOTECHNOLOGY

SUPERVISOR
Prof. Emel Baloğlu

ISTANBUL-2024

ACIBADEM MEHMET ALI AYDINLAR UNIVERSITY INSTITUTE OF HEALTH SCIENCES

IDENTIFICATION OF INTERACTION PARTNERS OF β1 SUBUNIT OF Na^+/K^+-ATPASE PUMP (NKA) IN IN-VITRO HYPOXIC CARDIOMYOCYTES

BEYZA GÜRLER

M.Sc. THESIS

DEPARTMENT OF MEDICAL BIOTECHNOLOGY

SUPERVISOR

Prof. Emel Baloğlu

ISTANBUL-2024

DECLARATION

I declare that this thesis work is my work, I had no unethical behavior at any stages from the planning to the writing of the thesis, I obtained all the information in this thesis in accordance with academic and ethical rules, and I cited all the information and comments that were not obtained with this thesis work, and I provided resources in the list of references. I also declare that there was no violation of any patents and copyrights during the study and writing of this thesis.

27/06/2024

Beyza Gürler

PREFACE AND ACKNOWLEDGEMENT

I would like to start by expressing my biggest gratitude to my advisor, Prof. Emel Baloğlu. She believed in me 4 years ago, when even I didn't believe in myself. She was always with me physically and spiritually throughout this process. After 4 years together, I realized that she always thought about my well-being at the end of the day. I owe most of my academic life and subsequent successes to her.

I would like to give another special thank you to my colleague Gizem Gençay. She always helped and supported me to learn everything she learned. She was a very good teacher and a best friend. I would also like to thank Aleyna Baltacıoğlu, Ufuk Amanvermez, İlayda Darılmaz, and Ayşegül Ekmekçioğlu for their extreme support and good memories and friendships throughout my graduate life.

Finally, I would like to thank my mother, father, and sister, who respect my targets throughout my life and tried to provide every opportunity and support me to achieve my dreams.

This project was supported by the Scientific and Technological Research Council of Turkey (TÜBİTAK) – 1001 Project (No: 119S688). I am grateful to TUBİTAK for financial support.

TABLE OF CONTENTS

LIST OF ABBREVIATIONS AND SYMBOLS

NKA	Sodium-Potassium ATPase
CVD	Cardiovascular Disease
RYR	Ryanodine Receptors
SR	Sarcoplasmic Reticulum
MLCK	Myosin Light Chain Kinase
SERCA	Sarcoendoplasmic Reticulum Calcium ATPase
ATP	Adenosine Triphosphate
NCX	Sodium–Calcium Exchanger
Ca-ATPase	Calcium-ATPase
Na^+/H^+	Sodium–Hydrogen Antiporter
Na^+/Mg^{2+}	Sodium-Magnesium Exchanger
Na^+/HCO_3^-	Sodium-Bicarbonate Cotransporter
$Na^+/K^+/2Cl^-$	Sodium-Potassium-Chloride Cotransporter
β1-NKA	β1 Subunit of Sodium-Potassium ATPase
α1-NKA	α1 Subunit of Sodium-Potassium ATPase
HIF	Hypoxia-Inducible Factor
MDCK	Madin-Darby Canine Kidney
PLM	Phospholemman
mRNA	Messenger Ribonucleic Acid
ATP	Adenosine Triphosphate
ARNT	Aryl Hydrocarbon Receptor Nuclear Translocator
bHLH	Basic Helix Loop-Helix
PAS	Per-ARNT-Sim
ODD	Oxygen-Dependent Degradation Domain
pVHL	Von Hippel-Lindau Tumor Suppressor Protein
N-TAD	N-terminal Transactivation Domain
C-TAD	C-terminal Transactivation Domain
PHD	Prolyl Hydroxylase Domain
HRE	Hypoxia Response Elements
VEGF	Vascular Endothelial Growth Factor

ANGPT1	Angiopoietin 1
ANGPT2	Angiopoietin 2
LDK1	Lactate Dehydrogenase
PDK1	Pyruvate Dehydrogenase Kinase 1
PDK3	Pyruvate Dehydrogenase Kinase 3
GLUT	Glucose Transporters
PPAR	Peroxisome Proliferator Activated Receptor
IGF-1	Insulin-Like Growth Factor
EPO	Erythropoietin
LDHA	Lactate Dehydrogenase A
TBS	Tris-Buffered Saline
TBST	Tris-Buffered Saline with 0.1% Tween 20
PBS	Phosphate-Buffered Saline
PBST	Phosphate-Buffered Saline with 0.1% Tween 20
CLB	Cell Lysis Buffer
IP-LB	Immunoprecipitation Lysis Buffer
WB	Wash Buffer
DMEM	Dulbecco's Modified Eagle Medium
EDTA	Ethylenediaminetetraacetic Acid
DMSO	Dimethyl Sulfoxide
GFP	Green Fluorescent Protein
HEK	Human Embryonic Kidney
MOI	Multiplicity of Infection
IP	Immunoprecipitation
NaCl	Sodium Chloride
SDS	Sodium Dodecyl Sulphate
PAGE	Polyacrylamide Gel Electrophoresis
Co-IP	Co-Immunoprecipitation
ECL	Enhanced Chemiluminescence
RGB	Resolving Gel Buffer
APS	Ammonium Persulfate

TEMED	Tetramethylethylenediamine
SGB	Stacking Gel Buffer
O/N	Overnight
RT	Room Temperature
BSA	Bovine Serum Albumin
LC/MS	Liquid Chromatography–Mass Spectrometry
WCL	Whole Cell Lysate
Hsp90β	Heat Shock Protein 90-Beta
Cav-I	Caveolin-I
Twf-I	Twiffilin-I

LIST OF FIGURES

LIST OF TABLES

ABSTRACT

Identification of Interaction Partners of β1 Subunit of Na^+/K^+-ATPase Pump (NKA) in in-vitro Hypoxic Cardiomyocytes

Optimal activity of the NKA pump in the heart is essential for maintenance of action potential, intracellular gradients, electrical coupling, and contractility. Pump activity reduced in samples from animal models and humans with heart failure. This causes intracellular Ca^{2+} overload, diastolic dysfunction and arrhythmia. Decreased NKA activity was associated with decreased expression of pump subunits. Hypoxia-inducible transcription factors (HIF), whose activity increases in ischemic heart, are crucial in the adaptation of cells to low oxygen conditions. The aim of this thesis is to determine the intracellular expression and interaction partners of the β1-NKA in in-vitro hypoxic/ischemic heart disease model, to investigate how the intracellular dynamics of β1-NKA regulated by hypoxia and the role of HIF-1α in this process. β1-NKA expression was measured in total cell lysates prepared from normoxic (~19%O_2), hypoxic (1%O_2) and HIF-1α gene expression silenced and non-silenced cells. Immunoprecipitation was performed using β1-NKA-specific antibody from the same lysates, and proteins interacting with β1-NKA and the signal transduction pathways they were involved in were identified through proteomic and bioinformatics analyses. These interactions confirmed by co-IP. Results showed that expression of mature form in ~42kD of β1-NKA increased HIF-1α dependent in hypoxia. Bioinformatics analyzes revealed that β1-NKA specifically interacts with Cav-I, Twf-I, and Hsp90β, which are involved in immune system, cellular stress, cell division and Golgi-ER transfer pathways. Interactions of these proteins with β1-NKA increased with hypoxia, while decreased in HIF-1α silenced cells. Future studies need to indicate whether these proteins play role in NKA activity via β1-NKA.

Keywords: Cardiac ischemia, Hypoxia, Hypoxia-inducible factors, Na^+/K^+-ATPase pump, β1 subunit of Na^+/K^+-ATPase.

ÖZET

In-vitro Hipoksik Kardiyomiyositlerde Na^+/K^+-ATPaz Pompasının β1 Alt Ünitesi ile Etkileşen Proteinlerin Saptanması

Kalpte NKA pompasının optimal aktivitesi aksiyon potansiyelinin, hücre içi gradyanların, elektriksel eşleşmenin ve kontraktilitenin korunması için gereklidir. Kalp yetmezliği olan hayvan modellerinden ve insanlardan alınan örneklerde pompa aktivitesi azalmaktadır. Bu azalma hücre içi Ca^{2+} yüklenmesine, diastolik disfonksiyona ve aritmiye neden olur. NKA aktivitesinin azalması pompa alt ünitelerinin ifadesindeki azalmayla ilişkilendirilmiştir. İskemik kalp hastalıklarında aktivitesi artan hipoksi ile indüklenebilir transkripsiyon faktörleri (HIF), hücrelerin düşük oksijen koşullarına adaptasyonunda önemli bir rol oynamaktadır. Bu tezin amacı, in-vitro hipoksik/iskemik kalp hastalığı modelinde β1-NKA alt ünitesinin hücre içindeki ifadesini ve etkileşim ortaklarını belirlemek, β1-NKAnın hücre içi dinamiklerinin hipoksi ile nasıl düzenlendiğini ve HIF-1α'nın bu süreçteki rolünü araştırmaktır. β1-NKAnın ekspresyonu normoksik (~%19O_2), hipoksik (%1O_2) ve HIF-1α gen ifadesi susturulmuş ve susturulmamış hücrelerden hazırlanan total hücre lizatlarında ölçüldü. Aynı lizatlardan β1-NKAya spesifik antikor kullanılarak immünpresipitasyon (IP) yapıldı, proteomik ve biyoinformatik analizlerle β1-NKA ile spesifik etkileşen proteinler ve dahil oldukları sinyal ileti yolakları tanımlandı. Bu proteinler co-IP ile doğrulandı. Sonuçlar β1-NKAnın ~42kDda görülen matur formunun ifadesinin hipokside HIF-1α aracılığıyla arttığını gösterdi. Biyoinformatik analizler β1-NKAnın bağışıklık sistemi, hücresel stres, hücre bölünmesi ve Golgi-ER transfer sistemi yolaklarında yer alan Cav-I, Twf-I, Hsp90β ile spesifik etkileştiğini ortaya çıkarttı. Bu proteinlerin β1-NKA ile etkileşimleri hipoksi ile artarken HIF-1α gen ifadesi silinmesi ile azaldı. Gelecek çalışmalarda bu proteinlerin β1-NKA aracılığı ile NKA aktivitesinde etkili olup olmadığının gösterilmesi gerekmektedir.

Anahtar Sözcükler: Kardiyak iskemi, Hipoksi, Hipoksi ile indüklenebilir faktörler, Na^+/K^+-ATPaz pompası, Na^+/K^+-ATPazın β1 alt ünitesi.

1 INTRODUCTION AND AIM

Ischemic heart diseases cover a wide range of diseases such as coronary artery diseases, hypertension, hypertrophic heart diseases, valve diseases, heart failure, pulmonary hypertension and anemia. Studies aimed at elucidating the changes that occur at the molecular and cellular level in the ischemic heart aim to contribute to the development of pharmacological treatment approaches that still have limited effectiveness.

In in-vitro and in-vivo cardiac ischemia models, autopsy materials of patients with heart failure it has been reported that the decrease in the expression of the Na^+/K^+-ATPase (NKA) pump subunits causes decrease in the pump activity, which has critical roles in the function of cardiomyocytes. Activation of hypoxia inducible transcription factors (HIFs), which cells developed as an adaptation mechanism for survival under different stress conditions, including low oxygen, increases in the ischemic heart. The starting point of our study was the unknown effect of HIFs on the intracellular dynamics of NKA pump subunits in the ischemic heart.

In the presented thesis, an in-vitro ischemic heart disease model created by keeping H9c2 rat ventricular cardiomyocyte cells in hypoxia ($1\%O_2$) for 24h. Studies have been conducted to understand how the β1-subunit, which plays a role in the localization of the catalytic α-subunit of the NKA pump to the cell membrane, regulated in the cell in cells with silenced HIF-1α gene expression. In this context, proteins interacting with β1-NKA identified by proteomics, comprehensive bioinformatics analyzes after immunoprecipitation, and the associated signaling pathways revealed.

Our results identified new proteins such as Hsp90β, Twifillin-I, and Caveolin-I that interact with the β1-NKA in hypoxic H9c2 cardiomyocytes, and the signaling pathways in which these proteins are involved in.

2 BACKGROUND

Cardiovascular diseases (CVD) account for approximately one-third of global deaths worldwide (1). Cardiac ischemia is the most prevalent disease among CVDs that manifests as ischemic cardiomyopathy and myocardial infarction. The increased incidence of CVD negatively affects the quality of life. Atherosclerosis, an inflammatory arterial disease associated with lipid accumulation and metabolic changes due to multiple risk factors, is the primary pathological process leading to ischemic heart diseases. It has been stated that more than 70% of individuals at risk, have more than one cardiac risk factor (2,3). Multiple therapeutic modalities, including surgical intervention, lifestyle modifications, pharmaceutical interventions, and cardiac rehabilitation, are available for management of the disease. However, the inadequacy of these strategies and the ever-increasing mortality rates emphasize the importance of developing new treatment approaches. In this regard, it is necessary to conduct research to better understand the physiopathology of CVDs (4).

2.1 Cardiac Ischemia

Cardiac ischemia refers to a pathological state characterized by insufficient delivery of oxygen and nutrients to the myocardium and removal of metabolic products (5). It can occur as short- or long-term. Temporary interruption of the heart's blood circulation is classified as short-term cardiac ischemia and usually does not damage the heart muscle unless it becomes chronic and recurs frequently (6). Prolonged cardiac ischemia, commonly caused by complete occlusion of the coronary arteries and can lead to permanent damage to the heart muscle, increases the activation of the Renin-Angiotensin-Aldosterone System and causes cardiac remodeling. For instance, increased Angiotensin II levels can lead to heart failure, increase in blood pressure, inflammation, and fibrosis (7). In cardiac ischemia, many metabolic changes also occur at the cellular level that impair cardiac function (8). Mainly, due to the accumulation of lactic acid, the cardiomyocytes become acidic, the pH and ionic balance is disturbed, along with decreased ATP production , increased glycolysis rate, oxidative stress, and intracellular Ca^{2+}, contributing to impaired contraction (9, 10).

2.2 Cardiac Cycle

The cardiac cycle is a process of sequential events that allow pumping oxygen and nutrients through contraction and relaxation of the heart. Disruptions of the critically maintained cycle may lead to the development of cardiac rhythm problems and associated cardiac diseases (11).

Cardiac impulses generated by the sinoatrial (SA) nodes, initiate action potential. The electrical impulse is propagated into atrioventricular (AV) node, then transmitted to ventricles via His Purkinje system(12). With the increase in membrane potential by the influx of Na^+ into the cell the action potential is transmitted through the sarcolemma to the T tubules, opening L-type voltage dependent Ca^{2+} channels. The increase in intracellular Ca^{2+} stimulates ryanodine receptors (RYR) in the sarcoplasmic reticulum (SR), increasing the Ca^{2+} released from the SR. Finally, the accumulated Ca^{2+} that inside the cell bind to the calcium-binding protein troponin, tropomyosin removed from actin, and cross-bridge between myosin and actin occurs. Increased intracellular Ca^{2+} also binds to calmodulin. Ca/calmodulin complex further activates myosin light chain kinase (MLCK), causing contraction (13, 14).

In the relaxation phase, Ca^{2+} ions are released from proteins from the myofilaments. Most of the released Ca^{2+} ions are taken back into the SR via the SERCA pump, rest of are released from cytosol via Na^+/Ca^{2+} exchanger (NCX) and Ca-ATPase, lowering the intracellular Ca^{2+} concentration and leading to relaxation (Figure 1) (12). Therefore, the balance of Ca^{2+} and Na^+ ion concentration in the cell is important for the heart to function properly.

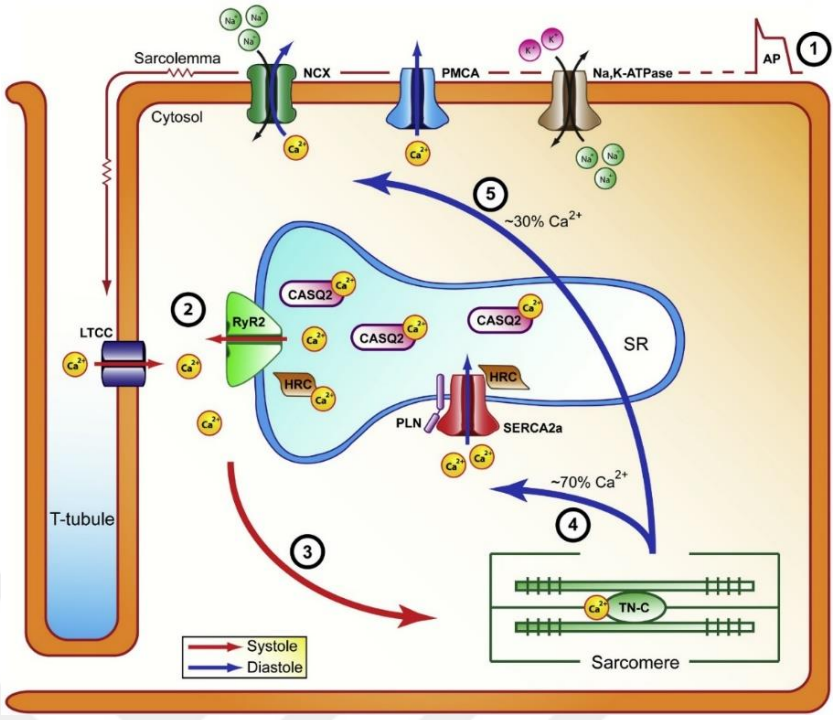

Figure 1. Regulation of intracellular Ca^{2+} in the systole and diastole phases of cardiac cycle (15).

There are other ion transporters and channels such as Na^+/H^+, NCX, Na^+/Mg^{2+} exchangers, voltage gated Na^+ channels, Na^+/HCO_3^- and $Na^+/K^+/2Cl^-$ cotransporters that allow Na^+ entry into the cell in myocytes. The only mechanism that ensures the excretion of Na^+ out of the cell is the Na^+/K^+-ATPase (NKA) pump. Since all these channels, cotransporters, exchangers and NKA pump work properly and in harmony with each other, and also affect the intracellular Ca^+ level in cardiomyocytes, any imbalance or malfunction in these mechanisms may adversely affect the functioning of the heart (14).

2.3 Structure of Na+ /K+ -ATPase (NKA) Pump

NKA is an enzyme and P-type ATPase pump in cell membranes that actively transports sodium (Na^+) and potassium (K^+) ions across the cell membrane (16). It affects many biological processes such as muscle contraction, intracellular volume control, action potential conduction in nerve cells by maintaining the electrochemical gradient of the cell membrane (17).

The NKA pump consists of α, β, and γ subunits which are responsible for the catalytic activity, regulation, and structural function of the enzyme, respectively. The structure of NKA is shown in Figure 2 (18).

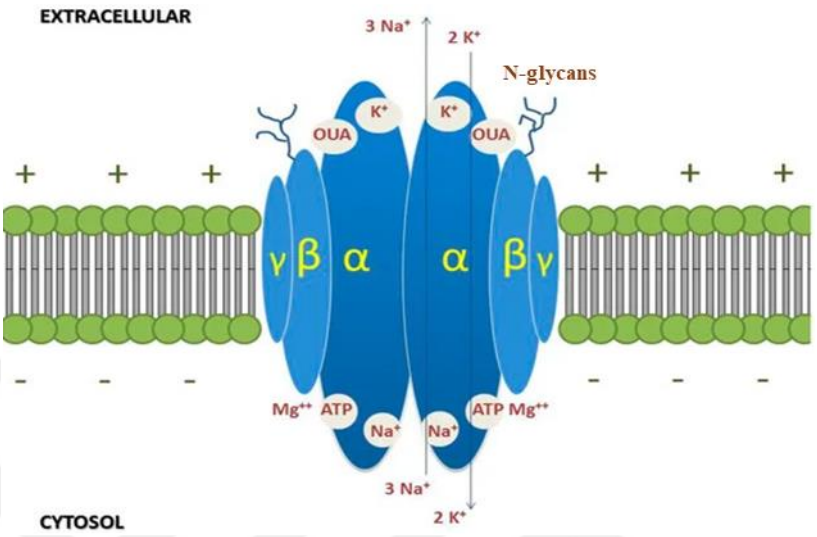

Figure 2. NKA pump structure. The α subunit has ATP, K^+, Mg^{2+}, Na^+, and ouabain binding sites, and β subunit has various sites of N-glycosylation (18).

The catalytic α subunit consists of ten transmembrane segments and has four different isoforms as α1, α2, α3, α4. These isoforms help regulating the Na^+ and K^+ transport to meet their tissue-specific needs. The localization and expression of alpha subunits are different in cells (19,20). For example, α1-NKA is found in all cells and is expressed in the T-tubules and cell membrane, whereas α2- and α3- isoforms are mostly expressed in the T tubules of the heart, brain, and skeletal muscle. The α4-isoform is found in the testicles and regulates sperm motility (21,22).

The β subunit of the NKA (β-NKA) is a single transmembrane protein, approximately 50-55kD in size, has three isoforms (β1, β2, and β3) (23). The N-terminal region of β1-NKA is located within the cytosol, while the C-terminal region is positioned in the extracellular region (24). The expression of β1-NKA vary among tissues in both glycosylated and non-glycosylated forms. N-glycans attached to the β subunit of the NKA play crucial roles in various aspects of pump function, including stable integration of the α subunit into the membrane, proper folding, stability, subunit assembly, and enzymatic activity. Functions of N-glycans of the β subunit are specific

to each isoform (25). For example, the level of endogenous β1 subunit was reduced in mutant epithelial MDCK cells lacking N-glycosylation sites of β1-NKA and the susceptibility to endocytosis was increased. It is suggested that the N-glycans of the β1-NKA subunit are essential for lateral membrane retention, maintaining pump localization at cell-cell contact sites, forming initial cell-cell junctions, adherens junction stability, and tight junction integrity (25,26). Although all three isoforms are expressed in the heart, the most studied isoform is β1-NKA due to its role in structural organization, membrane insertion of α1-NKA, and regulation of the NKA activity (27). It plays a crucial role as a molecular chaperone and controls the proper orientation of the α1 subunit. The β-NKA subunit, which is found together with different isoforms of the α subunit in the heart, is mostly found in combination with α1. While the affinity of the mutated β1 subunit to K^+ and ouabain is unaffected, its assembly with α-NKA is reduced and the susceptibility of the enzyme to proteolysis is increased (28, 29). In MDCK cells, while minor portion of the pump is present in the basal membrane, it is predominantly co-localized with β-catenin which is a marker of adherens junctions along the lateral membrane (23). The adherens junctions formed by E-cadherin/β-catenin complex rely on calcium for the stability. When MDCK cells are exposed to a calcium-free medium, intercellular junctions become disrupted, leading to cell separation and internalization of both NKA and junctional proteins (23,30).

The third subunit is identified as a γ subunit or a member of the FXYD family, which consists of a group of small membrane proteins comprising seven distinct members (FXYD1-7) (31). Phospholemman (PLM), a small protein member of FXYD1, mainly expressed in the heart have unique functions due to the multiple phosphorylation sites located at its cytosolic carboxyl terminus. It has crucial roles in regulation of NKA and SERCA pumps. Unphosphorylated PLM inhibits NKA activity by interacting with α and β subunits, thereby reducing their binding affinity for internal Na^+ ions (32,33).

2.4 Importance of NKA for Cardiomyocyte Function

The activity of NKA in cardiac muscle plays a crucial role in several physiological processes, including the generation of action potentials, regulation of electrical activity, establishment of Na^+ and Ca^{2+} ion gradients, and control of intracellular volume. Consequently, it helps maintaining the intracellular Na^+ concentration within certain limits, ensuring proper functioning of cardiac cells (34). NKA operates by pumping $3Na^+$ ions out of the cell and transporting $2K^+$ ions into the cell, utilizing the energy obtained from the hydrolysis of ATP molecules. This mechanism directly maintains cellular Na^+ and K^+ homeostasis and indirectly impacts Ca^{2+} homeostasis by regulating the function of NCX (35).

NCX exchanger operates by exchanging three Na^+ ions for one Ca^{2+} ion, serving as a crucial mechanism for excreting Ca^{2+} from cardiac myocytes (36). Unlike other Na^+ transporters, NCX has the unique ability to function in both extruding and allowing the influx of Ca^{2+}, depending on the concentrations of Ca^{2+} and Na^+ inside the cell. High level of intracellular Ca^{2+} promotes Ca^{2+} extrusion while high intracellular Na^+ enhance Ca^{2+} influx. Hence, the activity of NCX is regulated by the levels of Na^+ ions within the cell (37).

Cardiac NKA also acts as a receptor for cardiac glycosides which since a long time are used as positive inotropic drugs in the treatment of heart failure via binding to α1 subunit of NKA. Recent research has unveiled additional roles of NKA beyond its function as an ion transporter, demonstrating its involvement in intracellular signal transmission, and scaffold protein (38).

2.5 Regulation of NKA in Cardiac Ischemia

Understanding how NKA regulated in ischemic heart diseases is crucial due to its vital functions in myocytes. Numerous studies have observed a decrease in NKA activity in ischemic hearts tissues and animal models (39). Schwinger et al. demonstrated a 43% reduction in NKA activity and approximately 40% decrease in [3H]-ouabain binding in the left ventricles of individuals with heart failure.

Additionally, their study revealed decreased protein expression of α1-, α3-, and β1-NKA in the failing myocardium compared to non-failing myocardium. However, no significant alteration was observed in the protein levels of α2-NKA (40). Semb et al. demonstrated a reduction in the capacity of NKA without alterations in the mRNA and protein levels of α1- and β1-NKA in a rat model of hypertrophy and congestive heart failure following myocardial infarction. Their study revealed a shift in isoform expression from α2-NKA to α3-NKA, attributed to increased protein expression of α3-NKA (41).

Elevated intracellular Na^+ levels in cardiac ischemia, driven by increased activity of voltage-sensitive Na channels and Na^+/H^+ exchangers, surpass NKA activity. It also correlates with increased protein levels of phosphorylated PLM and its association with α subunits (42, 43). Increased Na^+ levels results in Ca^{2+} overload via NCX and decreased Ca^{2+} excretion. This causes impaired diastolic function, arrhythmias, compromised cell metabolism, and oxidative stress (44, 45). Cellular ATP levels typically decrease during ischemia, however it is not the primary factor imparing NKA activity. This is because NKA activity diminishes before cellular ATP levels decline, and the levels remain adequate to sustain NKA function (45, 46). Although it is common in various studies that NKA activity decreases, there are inconsistencies about the changes in the mRNA and protein levels of the NKA subunits that translates into decreased activity (47, 48).

Previous studies indicated that the expression of α1-NKA decreased both in the plasma membrane and intracellular fraction in hypoxia, an effect that completely prevented by silencing HIF-1α. Approximately 35% in the membrane expression of β1-NKA protein also decreased in hypoxia independent of HIF-1α. The intracellular expression of β1-NKA remained unaffected by either hypoxia or HIF-1α silencing (46). Together, it is unknown how β1-NKA is regulated in hypoxic cardiomyocytes and the proteins and signaling mechanism involved in remains to be identified.

2.6 Hypoxia and Structure of Hypoxia Inducible Factors (HIFs)

Molecular oxygen is essential for life, and for all mammalian cells at varying requirements for maintaining physiological homeostasis. Hypoxia is a condition in which inadequate oxygen level at the tissue level either due to low oxygen in blood or low blood supply (49). Diseases such as heart failure, arrhythmia, cardiac ischemia, asthma, and pulmonary hypertension are often related to tissue hypoxia. All cell types are sensitive to hypoxia, however their adaptation to hypoxia vary. Cells commonly shift from aerobic to anaerobic metabolism to provide ATP production and increase several physiological processes such as angiogenesis, respiratory rate, and erythrocyte production through the secretion of metabolites and hormones to enhance oxygen supply in low oxygen condition (50). Moreover, depending on the severity and duration of hypoxia, increased sympathetic system activity (51).

Hypoxia-inducible factors (HIFs) play a crucial role in adaption of cells to low oxygen levels by regulating the transcription and translation of different genes depending on the cell type and are involved in various pathological, physiological, and embryonic developmental processes in all eukaryotic cells (52). HIF has a heterodimer structure comprised of three subunits, oxygen- dependent α and oxygen-independent β or ARNT (aryl hydrocarbon receptor nuclear translocator). The HIF-α subunit exists in HIF-1α, HIF-2α, and HIF-3α isoforms and the HIF-β subunit has HIF-1β, HIF-2β, and HIF-3β isoforms (53, 54). Basic helix loop-helix (bHLH) and Per-ARNT-Sim (PAS) regions which are found in N-terminal of HIF subunits have role in the DNA binding and heterodimerization, respectively (55). The HIF-α subunits possess an oxygen-dependent degradation domain (ODD), which contains the region for recognizing the Von Hippel-Lindau tumor suppressor protein (pVHL) that mediates ubiquitin-mediated degradation, and the N-terminal transactivation domain (N-TAD) necessary for the activation of target genes. Additionally, both HIF-1α and HIF-2α possess a C-terminal transactivation domain (C-TAD) with a p300/CBP binding region (56, 57). Ubiquitously expressed HIF-β subunit lacks ODD domain and N-TAD, indicating oxygen-independency, and lack of transcriptional activity (58).

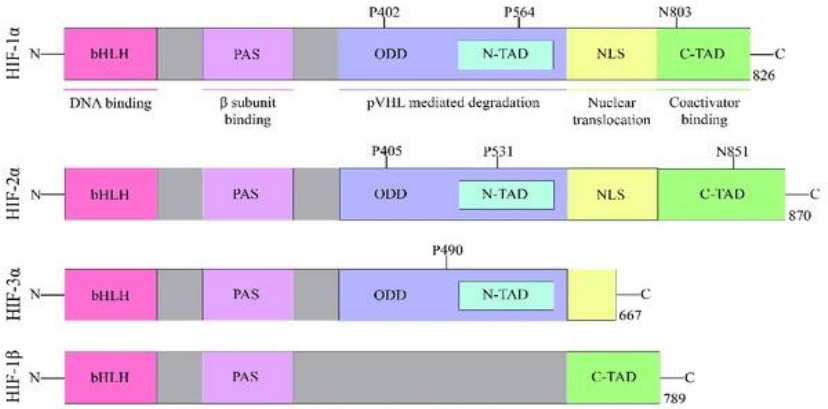

Figure 3. Domain structure of HIF subunit isoforms. bHLH represents basic helix loop-helix, PAS is Per-ARNT-Sim region, ODD is oxygen-dependent degradation domain, N-TAD is N-terminal transactivation domain, and C-TAD is C-terminal transactivation domain (50).

2.7 Regulation of HIF in Cardiac Ischemia

Regulation of HIF-α depends on the cellular oxygen level and any other stress conditions. (33, 59). HIF-prolyl hydroxylase (PHD) enzymes control HIF-α half-life, hydroxylate two proline residues in the ODD domain of HIF-α using molecular oxygen. Under normoxia, PHD enzymes rapidly hydroxylate HIF-α, followed by recognition of the hydroxylated subunit by pVHL. It then complexes with E3 ubiquitin ligase pVHL, tagging hydroxylated subunit with ubiquitin and resulting in HIF-α degradation by the 26S proteasome system. However, under hypoxia, PHD activity is suppressed, preventing the hydroxylation of HIF-1α and binding of pVHL to the HIF-α subunit. As a result, accumulated HIF-α becomes stabilized by forming a dimer with the HIF-β subunit together with p300/CBP co-activators and the complex is then transported to the nucleus and interacts with the hypoxic response element (HRE) region of specific genes, stimulating their transcription (56, 60).

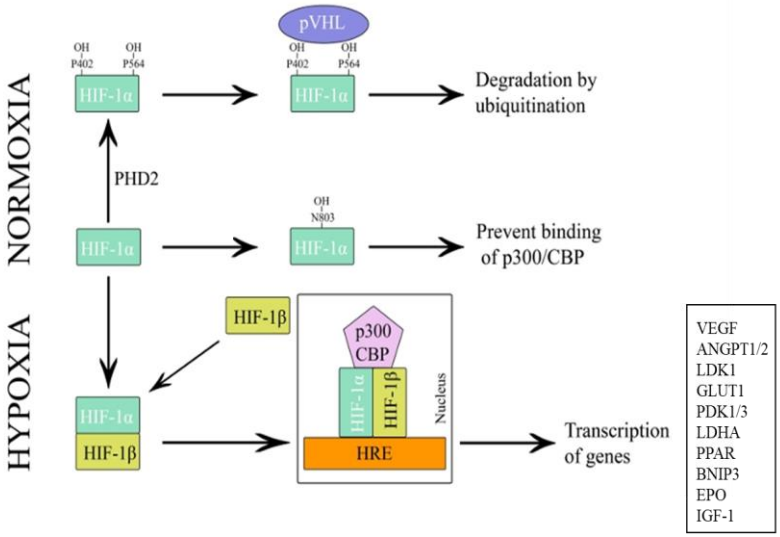

Figure 4. HIF regulation in normoxia and hypoxia. In normoxia, HIF-1α is degraded by ubiquitination, while in hypoxia it is stabilized, translocates into nucleus, and activates transcription of certain genes. Some of these genes are shown (50).

More than 1,000 human genes involved in various processes like angiogenesis, erythropoiesis, lipid synthesis, autophagy, and glucose transportation are regulated directly by HIF-1α (61, 62). Some of these genes are vascular endothelial growth factor (VEGF), angiopoietin 1 and angiopoietin 2 (ANGPT1/ANGPT2), lactate dehydrogenase (LDK1), pyruvate dehydrogenase kinase (PDK1/PDK3) glucose transporters (GLUT), peroxisome proliferator activated receptor (PPAR), insulin-like growth factor (IGF-1), erythropoietin (EPO), Lactate dehydrogenase A (LDHA), and Bcl-2/adenovirus E1B 19-kDa interacting protein 3 (BNIP3). Although HIF-1α and HIF-2α increase the transcription and protein synthesis of some genes, this effect may vary from cell to cell depending on the duration and severity of the hypoxia.

HIFs are also involved in organogenesis during embryonic development (63). During early embryonic stages, cardiomyocyte precursors rely on glycolytic pathways and pyruvate oxidation for energy. As the heart matures, there is a transition towards oxidative phosphorylation facilitated by increased mitochondrial development, to meet the increased energy demand (64). Adaptation of adult heart to ischemia initially involves maintaining intracellular ATP levels that achieved by redirecting the energy obtained from fatty acid beta-oxidation to glycolytic pathways. This metabolic shift, characterized by decreased beta oxidation enzyme expression, capacity and increased

glycolytic enzyme activity, aims to match the myocardial oxygen demand with supply (65, 66). In cardiac hypertrophy and heart failure caused by pressure and volume overload, similar metabolic shifts occur, by activated glycolytic metabolism due to elevated HIF-1α levels in human necropsy materials and mouse models (61, 67). However, this adaptive response has a dual impact on myocyte survival during stress. While short-term activation of HIF-1α indicates protective effects in cardiac hypertrophy and heart failure, prolonged HIF-1α activation may lead to adverse outcomes like apoptosis and cardiac decompensation, emphasizing the critical timing of HIF activity in adaptive responses during cardiac ischemia (67, 68). On the other hand, HIF-1α knock-down protected cardiomyocytes from apoptosis and contractile dysfunction (67).

Elevated HIF-α levels have been associated with various CVD such as cardiac hypertrophy, myocardial arrhythmia, and pulmonary hypertension (69). Agents like noradrenaline and angiotensin II, commonly used to simulate cardiac stress both in in-vivo and in-vitro cardiac ischemia and hypertrophy models, elevate HIF-1α levels and induce HIF-dependent metabolic changes contributing to cardiac remodeling (70, 71). These agents have also been implicated in regulating NKA activity in the ischemic heart, indicating a potential role of HIFs in regulating NKA. Recent reports showed that in in-vitro ischemic heart model hypoxia decreased the membrane expression of α1-and β1-NKA along with decreased NKA activity. HIF-1α silencing in hypoxic cells totally reversed decreased NKA activity (33, 46). The mechanisms of these observed effects on the expression profile of the NKA subunits is not known. This thesis investigated the role of HIF-1α in regulating the expression of β1-NKA and any potential interacting protein partners in in-vitro ischemic heart model.

3 MATERIALS AND METHODS

3.1 Materials

3.1.1 Buffers

10X Running Buffer: 144 g glycine, 10 g SDS, and 30 g Tris base were dissolved in 1L total volume of ddH_2O. pH was adjusted to 8.3 and kept at RT.

10X Wet Transfer Buffer: 144 g glycine and 40 g Tris base were dissolved in 1L total volume of ddH_2O. pH was adjusted to 8.3 and kept at 4°C.

10X Tris-Buffered Saline (TBS): 80 g NaCl and 24.2 g Tris base were dissolved in 1L total volume of ddH_2O. pH was adjusted to 7.6 and kept at RT.

1X Tris-Buffered Saline, 0.1% Tween 20 (TBST): 9 volume of ddH_2O was mixed with 1 volume of 10X TBS and Tween-20 was added at 0.1% final concentration.

10X Phosphate-Buffered Saline (PBS): 80 g of 1.37 M NaCl, 2 g of 24 mM KCl, 7.7 g of 43 mM Na_2HPO_4, 1.9 g of 14 mM KH_2PO_4 dissolved in ddH_2O at 1L final volume. pH was adjusted to 7.4 with NaOH and stored at RT.

Cell Lysis Buffer (CLB): 1% Triton X-100, 150 mM NaCl, 5 mM EDTA, 50 mM Tris (pH 7.5), 5% Glycerol, 1 mM $NaVO_3$, 1 mM PMSF, 1mM NaF, and 1X protease inhibitor cocktail. Final volume adjusted with ddH_2O.

Lysis Buffer for IP (IP-LB): 150mM NaCl, 50mM Tris (pH 7.5), 5mM EDTA, 0.5% Triton X-100 were mixed with ddH_2O and supplemented with 2mM Na_3VO_4, 2mM PMSF, 2X Roche protease inhibitor cocktail before use and kept on ice.

Wash Buffer for IP: 150 mM NaCl, 50mM Tris (ph 7.5), 1mM EDTA, 1% TritonX-100, 1mM PMSF. Final volume adjusted with ddH_2O.

Membrane Homogenization Buffer: 600 mM sucrose, 10 mM imidazole, pH 7.4

Membrane suspension Buffer: 250 mM sucrose, 30 mM imidazole, pH 7.4

3.2 Methods

3.2.1 Cell Culture experiments

3.2.1.1 Cell Culture maintenance

H9c2 (embryonic rat cardiomyoblasts) and HEK293T (human embriyonic kidney) cell lines purchased from ATCC were used. H9c2 cells were seeded in T75 cell culture flask and grown in complete Dulbecco's Modified Eagle Medium (cDMEM) containing 5mM HEPES, 1000mg/L glucose, 1mM sodium pyruvate, 4mM L-glutamine, 1X Penicillin-Streptomycin, and 10% fetal bovine serum (FBS). HEK293T cells were cultured with cDMEM containing 4500g/L glucose, 5 ml of 100X Penicillin-Streptomycin, 10mM HEPES, 2mM L-glutamine, 10% FBS, 1mM sodium pyruvate. Cells were grown in CO_2 incubator with 5% CO_2 at 37 °C. When the cells reached 80% confluency, cells were passaged. To harvest the cells, medium was aspirated, surface of the flask was washed with 5 ml of PBS, cells were incubated for 2-3 min with 3 ml of PBS - %0.01 EDTA - 1X Trypsin solution to cells detach. After the cells were detach, 7 ml of cDMEM was added to flask, cells were collected into a falcon by gently washing the surface of the flask several times and centrifuged at 500rpm for 5 min. Cell pellet was gently suspended with 1 ml of cDMEM and diluted in 1:2 ratio with trypan blue dye to count cells using hemocytometer.

3.2.1.2 Cell freezing and thawing

Approximately $2x10^5$ cells to be frozen were resuspended with 1 ml of cell freezing medium containing 10% DMSO and 10% FBS and kept in cryovials using Mr. Frosty box at -80 °C. After 48 hours, cryovials were transferred into liquid nitrogen for long-term storage. For thawing, cells were kept in water bath until almost all the cells dissolve and mixed with 9 ml of cDMEM, centrifuged at 500rpm for 5 min. After centrifuge, cell pellet was suspended with cDMEM and seeded in a T25 cell culture flask.

3.2.2 Silencing of HIF-1α gene expression

3.2.2.1 Amplification of adenoviruses

In this study, GFP-expressing adenoviruses containing shHIF-1α and control scrambled sequence against to the rat genome, which we generated from previous studies were used (71). To obtain high viral titers, adenoviruses were amplified using HEK293T cell line which has replicative E1 region (72). Cells were cultured in T75 cell culture flasks coated with type V collagen derived from rat tail for better attachment of the cells. In the subsequent days, cells were infected with adenoviruses at a multiplicity of infection (MOI) of 1. When cytopathic effect was observed with detachment of the cells from the surface of flasks, medium was collected and centrifuged at 2000g for 5 min at 4°C. The supernatant was discarded, and cell pellet was gently suspended in 2 ml of DMEM. To release the adenoviruses, cell suspension was vortexed, frozen, and thawed, and this step was repeated three times. Then, it was centrifuged twice at 20000g for 10 min, the supernatant containing adenoviruses was collected, and an equal volume of DMEM containing sterile 50% glycerol was added to the supernatant. Aliquoted adenoviruses were stored at -80°C until used.

3.2.2.2 End-point dilution assay for adenovirus titration

To determine adenovirus titration, $1x10^5$ HEK293T cells were cultured in 12-well plates coated with collagen in 500µl of medium. Various dilutions (1:40 to 1:1600) of adenoviruses were prepared through serial dilution, and 5 µl of these dilutions were added to the cells. After 24 hours, the GFP expression in the cells was examined under a fluorescent microscope, and the adenovirus titer was calculated using the formula below:

MOI/ml = original dilution x cell density x final dilution x 2,5 x % shining cell.

3.2.2.3 Adenovirus-mediated transfection and hypoxia experiments

Scrambled virus for control and adenovirus containing rat shHIF-1α were used to generate HIF-1α silenced and non-silenced cells under normoxic and hypoxic conditions. For this purpose, $6x10^5$ H9c2 cells were seeded into 10 cm dishes (4 nsv, 2 nh1, 2 hsv, 2 hh1 dishes) in 8 ml of cDMEM. Next day, cells were infected with 500 µL of adenoviruses in total 6 ml of transfection medium containing 10% FBS and without Penicillin-Streptomycin, at a concentration of 100MOI/cell. After 24h, transfection medium containing adenovirus was replaced with cDMEM and cells were incubated for 24h under normoxic and hypoxic conditions. Regular CO_2 incubator at ~19% O_2 for normoxia and oxygen-adjustable CO_2 incubator (Binder) at 1% O_2 at 37 °C for hypoxic conditions were used.

3.2.2.4 Preparation of whole cell lysate

Cells were washed three times with 1X ice cold PBS and aspirated thoroughly, 300µl of cell lysis buffer (CLB) was added to the cells, then cells were collected using a scraper and kept in 1.5 ml microcentrifuge tubes. Tubes were incubated on ice during 20 min by vortexing every 5 min. Then, tubes were centrifuged at 14000g for 10 min at 4°C and supernatants were collected in new microcentrifuge tubes. Lastly, protein concentrations were measured with Bradford assay (Bio-Rad) and stored at -80 °C until use.

3.2.3 Immunoprecipitation (IP) experiments for proteomics studies

Immunoprecipitation (IP) experiments followed by proteomic analysis were performed to determine proteins interacting with β1-NKA. Freshly prepared total whole cell lysates from normoxic and hypoxic cells with or without silencing HIF-1α were prepared as discussed above and used. Protein A Agarose beads (Praesto Jetted A50, Purolite) were used for IP experiments. Approximately 1400µl of beads were centrifuged at 500g for 30 sec at 4°C. Supernatant was discarded, PBS was added equal to the bead volume, and centrifuged again. This washing step was repeated three times. As a final wash, the beads were washed once with cell lysate buffer. To obtain 50%

Protein A Agarose beads, immunoprecipitation lysate buffer (IP-LB) was added at a volume equal to the bead volume.

To prevent non-specific binding, a preclearing step was performed. For preclearing, 600µg of total cell lysates from each conditions were mixed with 50µl Protein A Agarose beads and total volume was adjusted to 500µl with IP-LB. Mixtures were gently rotated at 10rpm for 30 min, centrifuged at 1000g for 2 min at 4°C, and supernatants were collected. After preclearing, 6µg of primary β1-NKA antibody (Proteintech, rabbit, 15192-1-AP) was added to pre-cleaned lysates, and rotated at 10rpm for 30 min at 4°C. Also, normoxic scrambled virus lysates with 6µg rabbit IgG antibody (Cell Signaling Technology, #2729) for positive control and without antibody for negative control were used. Then, 250µl of Protein A Agarose beads were added, total volume was adjusted to three times the bead volume with IP-LB, and rotated at 10rpm for 2 h at 4°C. Samples were centrifuged at 2000g for 2 min at 4°C, supernatants were collected, and shown as S. For washing step, 750µl of wash buffer was added and centrifuged at 2000g for 2 min at 4°C again. This step was repeated three times, supernatants from each wash fractions were collected and shown as W1 and W2. Lastly, beads were washed once with 750µl of 150 mM NaCl and 50mM Tris solution. To elute antibody bound proteins, the bead pellets were mixed vigorously with 500ul of 0.1M Glycine (pH: 2.2) for 5 min at RT. Samples were centrifuged at 2000g for 2 min at 4°C, supernatants were collected, and shown as E1 fraction. This step was repeated one more time (E2) and the pH of the elution fractions were neutralized with 125µl of Tris-base. For LC/MS analysis, 400µl of the E1 and E2 fractions were mixed, and the rest of fractions were stored at -80°C. To examine the IP efficiency, elution fractions along with pre-cleared cell lysates, and wash fractions were run on SDS-PAGE and Western Blot were performed.

3.2.4 Proteomics studies to identify interaction partners of β1-NKA

Hypoxia and HIF-1α-induced changes in the protein interaction network of β1-NKA were investigated by proteomics studies conducted at TUBITAK-UME using IP samples which were prepared before (E1+E2). In summary, protein levels in the IP elution fractions were measured for both the antibody control (empty bead) and the

β1-NKA antibody-treated samples using the QubitTM Protein Assay. Peptides were obtained through the FASP Protein Digestion Kit (Expedeon), following the manufacturer's protocols. Disulphide bonds of proteins were cleaved, and samples were washed with urea and ammonium carbonate solutions. Subsequently, peptides were separated using reverse-phase NanoLC liquid chromatography before being subjected to mass spectrometer analysis. For the analysis, Thermo Scientific ™ UltiMate ™ 3000 RSLC Ultra Nano ultra-performance liquid chromatography and Thermo Scientific Q Exactive ™ HF mass spectrometry was employed. Mass data analysis was carried out using TraceFinder ™ and Proteome Discoverer 2.4 software, referencing the NCBI Rattus Norvegicus (Rat) taxonomy (Taxonomy No: 10116).

3.2.5 Comparative group analysis

Proteome Discoverer 2.4 was employed for a quantitative and comparative analysis of the interactomes. Each elution fraction underwent a thorough examination three times, and peptides identified in at least two analyses were incorporated to reduce the likelihood of technical false negatives. The proteins identified in the treatment sets were categorized into distinct groups, and comparative analyses were conducted on the raw data. Empty bead-to-sample ratio of 0.5 was used to eliminate nonspecific outcomes. The entire process, from experiments to analysis, was replicated across three independent IP preparations.

3.2.6 Bioinformatics analysis

The data obtained from proteomic analyzes were analyzed with bioinformatics approaches. For proteins interacting with β1-NKA (Atp1b1), pathway enrichment analyzes were performed using REACTOME and KEGG data base (73) and Search Tool for the Retrieval of Interacting Genes/Proteins STRING (74, 75) to reveal protein-protein interactions and inter-protein relationships to identify cellular functions, signal transduction, and biological processes. Interaction networks were visualized with Cytoscape software, an open source data visualization and network analysis program in the fields of bioinformatics and systems biology, which is

frequently used to visualize and analyze large and complex biological data such as protein-protein interaction networks (76, 78).

3.2.7 Co-immunoprecipitation (Co-IP) experiments

According to the proteomics results, co-IP experiments were performed to confirm the proteins detected interacting with β1-NKA. These proteins included α1-NKA and Hsp90β. In these experiments, a protocol with slight modifications than the IP protocol mentioned above was applied optimization experiments.

To demonstrate Hsp90β and β1-NKA interaction, 25% slurry Protein A/G PLUS-Agarose beads (Santa Cruz, sc-2003) was used. Beads were spun down at 3500g for 3 min at 4C and washed three times with PBS and once with IP-LB adjusted 4-fold of bead volume. To obtain 50% slurry of Protein A/G Agarose beads equal amount of IP-LB was added according to bead volume, preclearing step was performed to prevent non-specific binding. For preclearing, 500µg whole cell lysates were mixed with 30µl of beads and rotated at 10rpm for 30 min at 4°C, centrifuged at 14000g for 10 min at 4°C. Supernatants were collected and protein levels were measured with Bradford assay. Then, 500µg of pre-cleared whole cell lysate from samples were mixed with 7µg of primary Hsp90β antibody (Abcam, rabbit, ab203085) at 1/42 dilution. Also, normoxic scrambled virus lysates with 7µg rabbit IgG antibody (Cell Signaling Technology, #2729) at 1/70 dilution for positive control and without antibody for negative control were used. Total volume of IP samples was adjusted to 300µl with IP-LB and rotated O/N at 10rpm at 4°C. Next day, 30µl of beads were added to samples and rotated 2h at 10rpm at 4°C. Samples were centrifuged at 3500g 4C for 3 min, 100µl were separated from the supernatants. (S). Remaining supernatants were washed six times with 1 ml of IP wash buffer (IP-WB). Wash fractions from the first and second wash were collected for testing. After last wash, samples were centrifuged one more time at 3500g for 3min at 4C and WB was removed by pipetting. Bead pellets were mixed with 30µl of 3X sample buffer (+ 5%mercaptoethanol), samples were denatured at 95°C for 5 min. To assess IP efficacy, 10 µg of pre-cleared whole cell lysates and elution fractions from each condition were run on 12% gel and incubated

with primary Hsp90β (1:40000, Abcam, rabbit, ab203085) and β1-NKA (1:3000, Proteintech, rabbit, 15192-1-AP) antibodies for O/N at 4°C.

To demonstrate α1- and β1-NKA interaction, the same protocol as above was applied with some modifications. For this experiment, 750µg of pre-cleared whole cell lysates were mixed with 3µg of primary α1-NKA antibody (Abcam, mouse, ab7671) and 3µg of mouse IgG antibody (Cell Signaling Technology, #5415), the total volume was made up to 970µl with IP buffer and rotated at 10rpm for 1.5h with over-end-rotator. At the end of the period, 30µl of 50% beads was added to the tubes and were rotated for 2h. After the last washing step, 15µl 4X SB (+10% mercaptoethanol) was added to the bead pellets. Samples were denatured at 37°C for 30 min for α1-NKA expression. Then, 10µg pre-cleared whole cell lysates, 1µl elution fractions, and 12µl supernatant fractions were run on 12% gel, membrane was incubated O/N with the primary α1-NKA antibody (1:2000, Abcam, mouse, ab7671). For β1-NKA expression, the samples were denatured at 95°C for 5 min. 25µg pre-cleared whole cell lysates and 9µl elution fractions were run, membrane was incubated O/N with primary β1-NKA (1:3000, Proteintech, rabbit, 15192-1-AP) antibody.

3.2.8 Preparation of membrane and whole cell lysate

Since Caveolin-I (Cav-I) is a membrane protein and is highly abundant in the membrane, its expression was examined in both whole cell lysates and membrane fractions. To prepare membrane, H9c2 cells from each conditions (nsv, nh1, hsv, hh1) washed three times with ice-cold PBS and scraped in 1 ml PBS. Collected cells were centrifuged at 1000g for 5 min at 4°C. Supernatants were aspirated and 1.2 ml of homogenization buffer composed of 600 mM sucrose, 10 mM imidazole at pH 7.4 was added to the cell pellets. Cells were incubated on ice for 30 min, passed 15 time through needle, and the centrifuged at 2000g for 5 min at 4°C. Supernatants were collected in new microcentrifuge tubes and centrifuged at 20000g for 30 min at 4°C. Supernatants were aspirated and pellets were suspended in membrane suspension buffer composed of 250mM sucrose, 30mM imidazole at pH 7.4 according to pellet volume. Then, protein concentrations were measured with Bradford assay and proteins were aliquoted at a final concentration of 1µg/µl. To prepare whole cell lysates for

Caveolin-I, $2x10^5$ cell was seeded in 6 cm dishes. Cells were infected with scrambled virus and shHIF-1α, and underwent normoxic and hypoxic conditions as mentioned above. Then, cells were washed three times with ice-cold PBS and 200µl of 1X Laemmli sample buffer containing 2.5% mercaptoethanol was added. Cells were scraped into microcentrifuge tubes and sonicated to shred DNA and spun down at 5000g for 3 min.

3.2.9 SDS-PAGE and western blot experiments

For SDS-PAGE and Western Blot experiments, 10% or 12% of SDS-PAGE gels were used according to the recipes given in Table 1 and Table 2. Proteins were run at 80V-100V, gels were transferred by wet blotting onto nitrocellulose membranes at 65V for 90 min at 4°C, and Ponceau staining was performed to confirm blotting efficiency. Enhanced chemiluminescence (ECL) reagent (Amersham) and ChemiDoc Imaging System (Biorad) were used for imaging. Band densities were normalized to β-actin (1:10000, Sigma, mouse, cat no: A2258) band densities using ImageJ free software.

Table 1: Recipe of resolving (lower) gels.

10% Resolving Gel	**2 gels**	**12% Resolving Gel**	**2 gels**
	volume (ml)		**volume (ml)**
ddH_2O	4,12	ddH_2O	2,75
RGB (1.5M Tris pH:8.8)	3,75	SGB (0.5M Tris pH:6.8)	3,75
10% SDS	0,15	10% SDS	0,15
30% Acrylamide	4,87	30% Acrylamide	5,84
2% Bis-Acrylamide	1,95	2% Bis-Acrylamide	2,34
10% APS	0,15	10% APS	0,150
TEMED	0,015	TEMED	0,015

Table 2: Recipe of stacking (upper) gel.

4% Stacking Gel	**2 gels**
	volume (ml)
ddH_2O	4,09
SGB (0.5M Tris pH:6.8)	1,89
10% SDS	0,075
30% Acrylamide	0,97
2% Bis-Acrylamide	0,39
10% APS	0,075
TEMED	0,0075

To evaluate the efficacy of HIF-1α silencing we examined the HIF-1α expressions. For HIF-1α Western Blot experiments 20µg of total protein was loaded on gels. After blotting membranes were incubated with 5% BSA-TBST for 30 min at RT for blocking, and washed 3 times for 5 min with 1X TBST. Membranes were incubated overnight at 4°C with HIF-1α (1:1000, Cell Signaling, rabbit, cat no: D2U3T, #14179S) primary antibody. Next day, membranes were washed, incubated with anti-rabbit (Calbiochem, 1:2000, cat no: DC03L) antibody for 1h at RT.

To assess IP efficacy and co-IP experiments, 10µg of pre-cleared whole cell lysates were run on 12% gel. For β1-NKA protein, membranes blocked with 5% MTBST for 1h at RT, incubated with primary β1-NKA (1:3000 in 5% MTBST, Proteintech, rabbit, 15192-1-AP) antibody O/N at 4°C, and Veriblot (1:500 in TBST, Abcam, ab131366) as secondary antibody was applied for 1h at RT. For Hsp90β co-IP experiments, membranes were blocked with 5% BSA+TBST for 30 min at RT, incubated with primary Hsp90β (1:40000 in TBST, Abcam, rabbit, ab203085) or β1-NKA antibodies O/N at 4°C, and anti-rabbit (1:2000 in TBST, Calbiochem, cat no: DC03L) secondary antibody. For α1-NKA co-IP experiments, membranes were blocked with 5% BSA+TBST for 30 min at RT, incubated with primary α1-NKA (1:2000 in 3% BSA+TBST, Abcam, mouse, ab7671) or β1-NKA for O/N at 4°C, and anti-mouse (1:4000 in TBST, Cell Signaling, #7076) antibodies.

To check the membrane expression of Caveolin-I, 10ug of H9c2 membranes were used for Western Blot experiments. After blotting, membranes were blocked with 7.5% MTBST O/N at 4°C. Next day, membranes incubated with primary Caveolin-I (1:200 in 5% MTBST, Santa Cruz, mouse, sc70516) for 1.5h at RT, and anti-mouse (1:4000 in TBST, Cell Signaling, #7076) antibodies.

3.2.10 Statistical analysis

Band densities of protein expressions measured from total cell lysates and membranes were normalized to beta actin band density analyzed by ImageG free software. Data are presented as mean ± standard deviation. Original data were analyzed by one-way ANOVA and differences between groups by Fisher's LSD posthoc test. T-test was used in the analysis of some results. $p < 0.05$ were considered statistically significant. Sigma Stat3.5 (Germany) was used to perform statistical analysis.

4 RESULTS

4.1 Efficiency of Adenovirus-Mediated HIF-1α Gene Silencing in H9c2 Cells

Western blot results in Figure 5 confirmed that HIF-1α is not expressed in normoxia and HIF-1α expression increased in hypoxia. Silencing HIF-1α with adenoviruses containing shHIF-1α almost completely inhibited the HIF-1α expression. These results revealed that HIF-1α silencing efficiency was ~100% ($p < 0.001$).

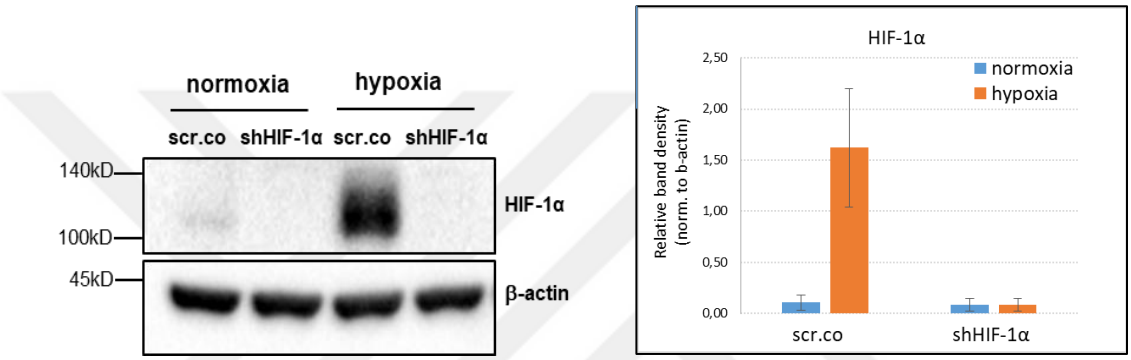

Figure 5. Efficiency of HIF-1α silencing on the expression of HIF-1α protein. H9c2 cells were infected with scrambled control and shHIF-1α containing adenoviruses at 100MOI, kept in normoxia (~19% O_2) or hypoxia (1% O_2) for 24h. HIF-1α band densities were normalized to β-actin. scr.co: scrambled control infected cells, shHIF-1α: HIF-1α silenced cells.

4.2 Effect of Hypoxia and HIF-1α Silencing on the Expression of β1-NKA

In whole cell lysates β1-NKA is expressed around both 42kD and 60kD as shown in Figure 6A. In line with the reports in literature β1-NKA has different molecular weights due to post-translational modifications. The expression of the band at 60kD did not change in normoxic or hypoxic control cells treated with shHIF-1α (Figure 6A, C). However, the expression of the band at ~42kD in hypoxic control cells increased compared to normoxic controls (Figure 6A, B, $p < 0.001$). This effect was abolished in hypoxic HIF-1α silenced cells (Figure 6A, B, $p < 0.001$) at a level comparable to the expression level in normoxic cells. These data suggest that hypoxia did not affect the expression of post-translational modification observed at 60kD, however mature form of the protein increased in hypoxia HIF-1α dependent manner.

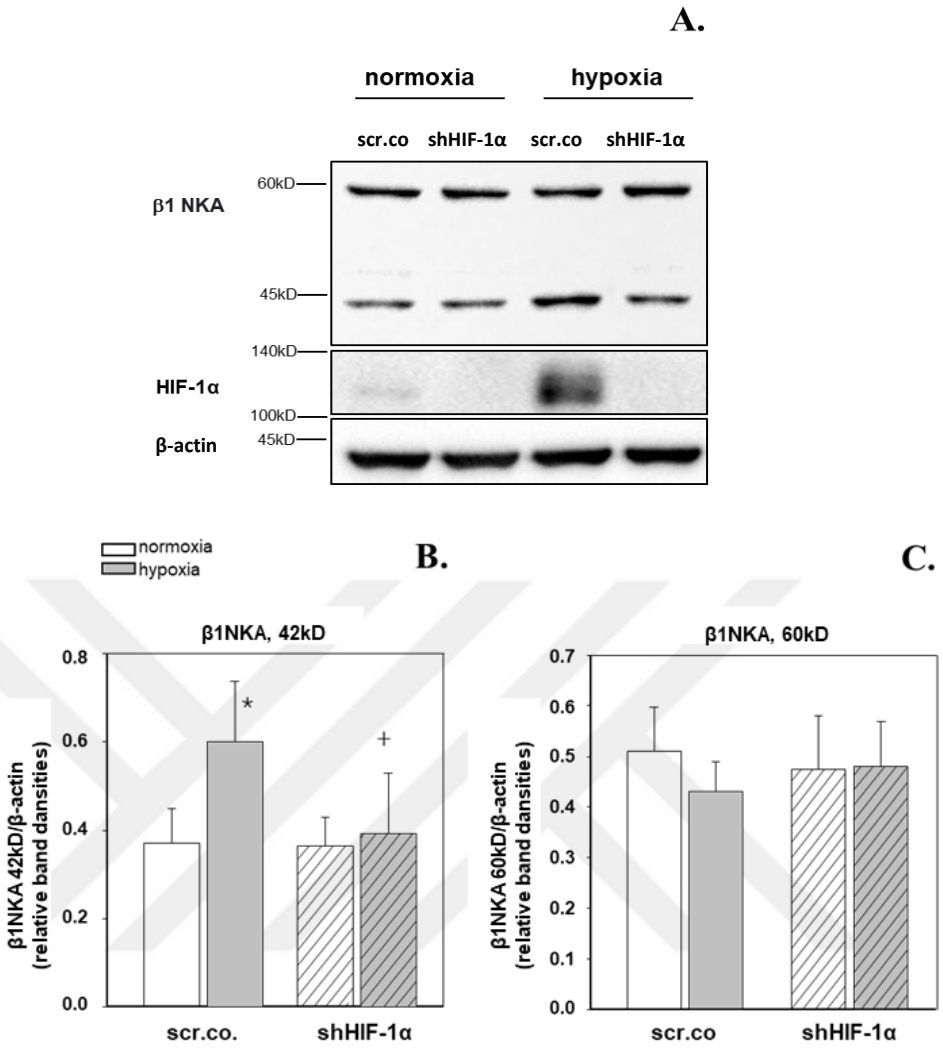

Figure 6. Expression of β1-NKA in whole cell lysates from normoxic, hypoxic, and HIF-1α silenced cells. β1-NKA band densities were normalized to β-actin, n=6. The significance level was $p < 0.05$:* effect of hypoxia compared to normoxia, $^{+}$ effect of HIF-1α silencing in hypoxia compared to hypoxic control cells. scr.co: scrambled control, shHIF-1α: HIF-1α silenced cells.

4.3 Immunoprecipitation (IP) Experiments for LC/MS Studies

IP experiments to detect interaction partners of β1-NKA using proteomics studies was performed. Prior to performing LC-MS/MS studies, IP efficiency was evaluated and a representative Western Blot image is given in Figure 7.

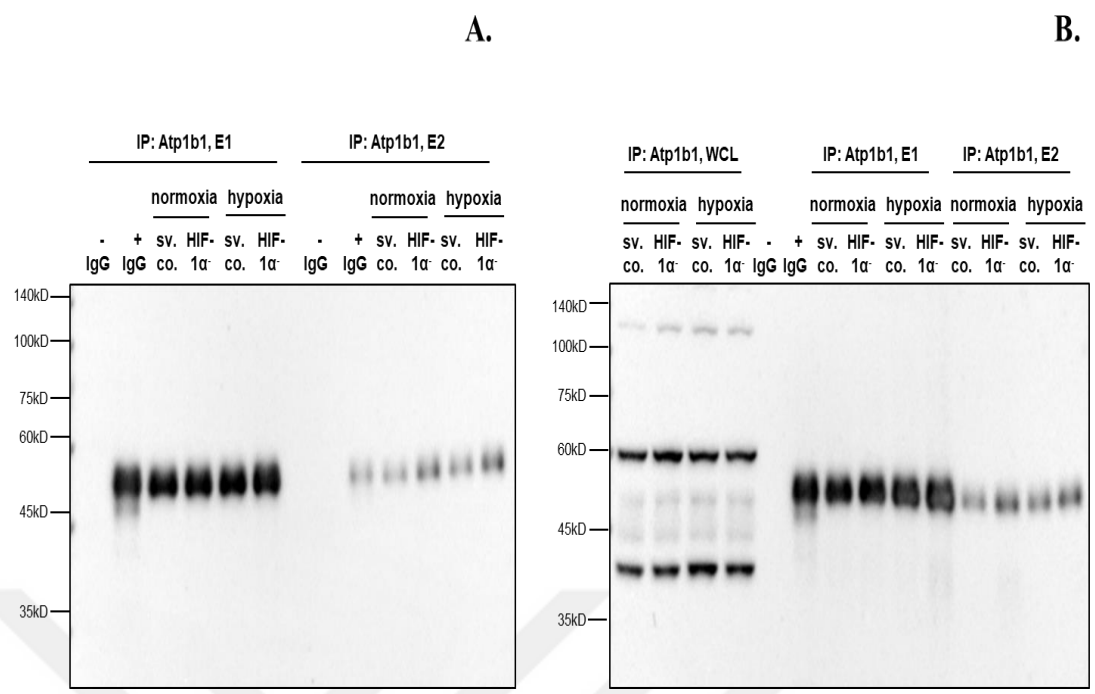

Figure 7. Evaluation of IP efficiency for proteomics studies. Pre-cleared WCL along with elution fractions were run SDS-PAGE. Blotted membrane was only incubated with HRP-coupled secondary antibody (A). Membrane incubated with primary β1-NKA and HRP-coupled secondary antibodies (B). -IgG: no isotype specific antibody, +IgG: isotype specific mouse antibody, E1: elution fraction 1, E2: elution fraction 2, WCL: whole cell lysate.

Figure 7A shows that primary β1-NKA and control antibodies were effectively collected from Protein A Agarose beads, with the majority of them in the E1 fraction compared to E2 fraction on the membrane incubated with only the secondary antibody. These results indicated that IP was performed successfully. After confirming IP efficiency, these samples were analyzed by proteomic studies and bioinformatics approaches from three experiment set, interaction partners of β1-NKA was determined, analyzed, and visualized.

The list of all Atp1b1 (β1-NKA) binding partners obtained from the three experiment groups and the genes this list shares under relevant experimental conditions are given in Table 3. Accordingly, in experiments performed from three different sets, 2 proteins were identified as Atp1b1 binding partners in common, 18 common partners were found in the experiment, which was conducted in at least two

sets. Also 81 proteins were determined to interact with Atp1b1 in only one experiment set. This data was shown as Venn diagram in Figure 8.

Table 3: List of genes interacting with Atp1b1 based on the analysis of three independent IP experiments.

Set	Gene	Gen Number
1 2 3	Cav1, Twf1	2
1 2	Klhl22, Hadhb, Tubb5, Hsp90ab1	4
1 3	Sord, Dctn2, Dctn4, Hspa5 , Dctn1, Actr1a, Ywhaz, Pdlim7, Capzb, Dpysl3, Anxa2, Htra1, Atp5f1a	13
2 3	Plec	1
1	Npm1, Vapb, Csrp1, Anxa1, Pkm, Eef2, Idh3a, Dars1, P4hb, Capza1, Nes, Mdh2, Capza2, Eif2s3, Hnrnpk, Hspa1a, Serpinh1, Tagln, H4c16, Myh7, Bcar3, Eif2ak4, Slc27a2	23
2	Tubb4b, Mapk1, Lyar, Myh4, Myl9, Slc25a3, Slc25a5, Actn1, Slc25a4, Csnk2a1, Sgpl1, Pecam1	12
3	Nono, Thrap3, Acbd5, Pyroxd2, Pabpc1, Cavin3, Cfl1, Serbp1, Ywhag, Dpysl2, Ywhab, Coro1b, Cavin2, Cav3, Hspa8, Usp28, Arhgef11, H1-4, Arf4, Atp1b1, Ywhah, Snrpb, Slc38a2,Dync1h1, Dab2ip, C4, Arglu1, Actb, Purb, Ago2, Vim, Cat, Cald1, Fxr, Eef1a1, Tubb2a, Mea1, Tjp1, C1qc, Mvp, Ywhae, Cavin1, Zc3h18, C3, Tuba4a, Rnh1	46

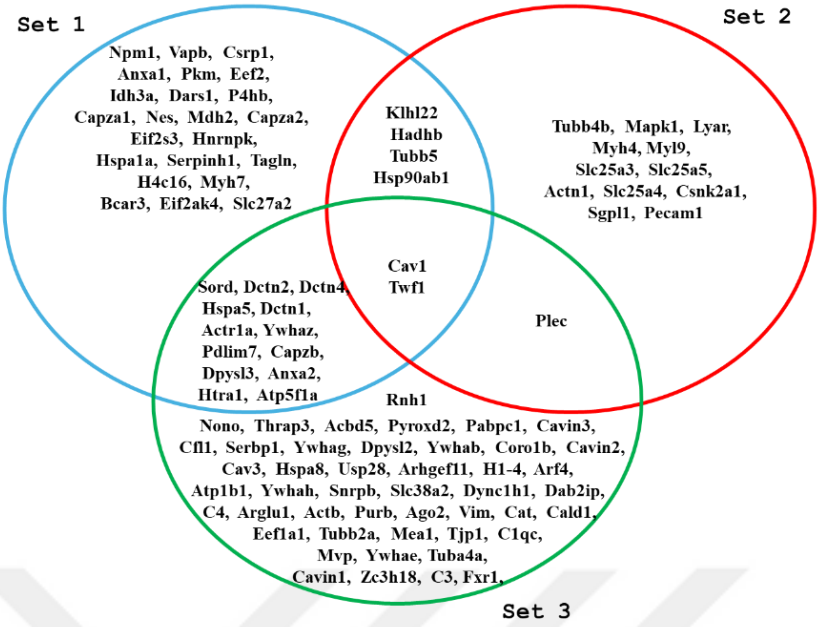

Figure 8. Venn diagram of Atp1b1 interacting proteins from different three sets of experiment.

Pathway enrichment analysis of Atp1b1-interacting proteins was performed using STRING and Reactome databases. The pathway list in Figure 9 includes remarkably pathways such as the immune system, different pathways related to cellular stress, retrograde transfer between Golgi-ER and cell division under cellular stress conditions.

The gene list detected in the pathway enrichment analysis shown in Figure 9 is listed in Table 4. Accordingly, it has been observed that protein partners such as Hsp90ab1 (Hsp90β) and Ywhaz (proteins including 14-3-3 subunits) are present in stress pathways. Additionally, it was noted that Tubb5, Dctn2, Actr1a, Dctn1 proteins were found especially in cell cycle-related pathways. One of the important interaction partners appeared in three IP analysis is Cav-I, which is responsible for the optimal function of many proteins such as receptors and enzymes in the cell membrane.

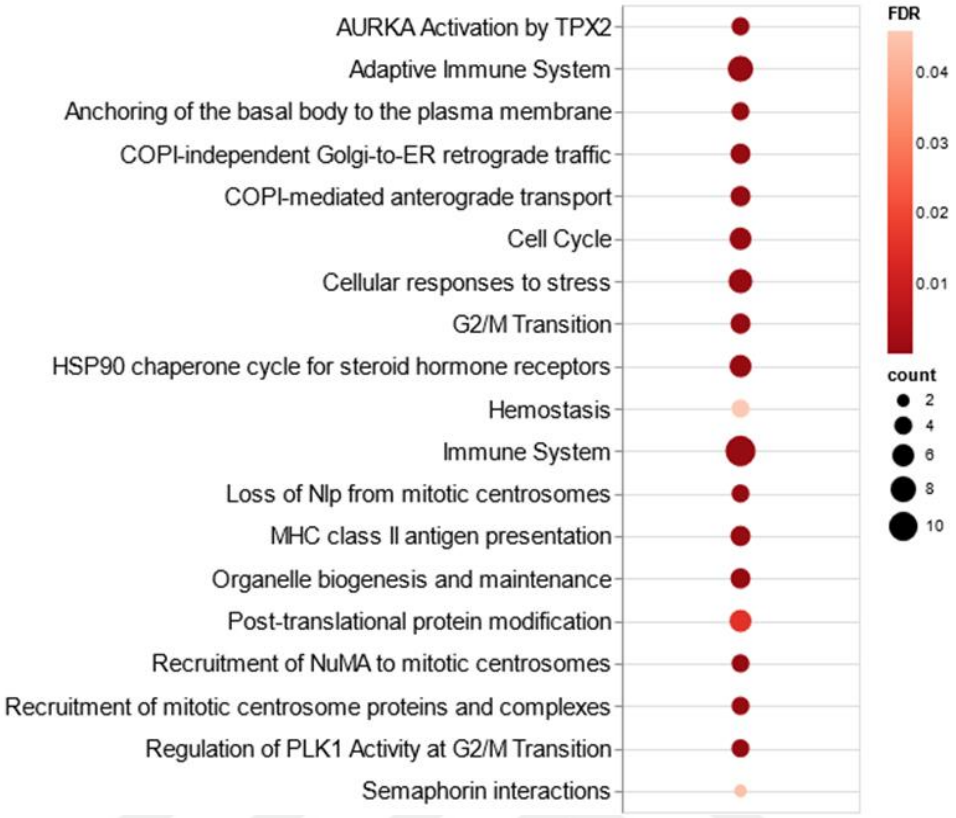

Figure 9. Pathway enrichment analysis of partners of Atp1b1. Reactome pathway of Atp1b1 interactome in HIF-1α silenced and control cells in normoxia and hypoxia was obtained using STRING and Reactome databases.

Table 4: List of genes identified in pathway enrichment analysis.

Reactome Pathway	**Atp1b1 Interaction Partners**
HSP90 chaperone cycle for steroid hormone receptors	Dctn2, Capzb, Dctn4, Actr1a, Hsp90ab1, Dctn1
COPI-independent Golgi-to-ER retrograde traffic	Dctn2, Capzb, Dctn4, Actr1a, Dctn1
Immune System	Tubb5, Dctn2, Capzb, Hspa5, Dctn4, Actr1a, Hsp90ab1, Ywhaz, Anxa2, Dctn1, Klhl22
COPI-mediated anterograde transport	Dctn2,Capzb,Dctn4,Actr1a,Dctn1
Cellular responses to stress	Dctn2, Capzb, Hspa5, Dctn4, Actr1a, Hsp90ab1, Dctn1
Adaptive Immune System	Dctn2, Capzb, Hspa5, Dctn4, Actr1a, Ywhaz, Dctn1, Klhl22
MHC class II antigen presentation	Dctn2,Capzb,Dctn4,Actr1a,Dctn1
Loss of Nlp from mitotic centrosomes	Tubb5,Dctn2,Actr1a,Dctn1
G2/M Transition	Tubb5, Dctn2, Actr1a, Hsp90ab1, Dctn1
AURKA Activation by TPX2	Tubb5, Dctn2, Actr1a, Dctn1
Recruitment of mitotic centrosome proteins and complexes	Tubb5, Dctn2, Actr1a, Dctn1
Regulation of PLK1 Activity at G2/M Transition	Tubb5, Dctn2, Actr1a, Dctn1
Recruitment of NuMA to mitotic centrosomes	Tubb5,Dctn2,Actr1a,Dctn1
Organelle biogenesis and maintenance	Tubb5,Dctn2,Atp5a1,Actr1a,Dctn1
Anchoring of the basal body to the plasma membrane	Tubb5, Dctn2, Actr1a, Dctn1
Cell Cycle	Tubb5, Dctn2, Actr1a, Hsp90ab1, Ywhaz, Dctn1
Post-translational protein modification	Dctn2, Capzb, Dctn4, Actr1a, Dctn1, Klhl22
Semaphorin interactions	Dpysl3, Hsp90ab1
Hemostasis	Cav1, Capzb, Ywhaz, Anxa2

According to the protein-protein interaction network in Figure 10, interaction of the Htra1 partner is reduced in hypoxic HIF-1α silenced cells compared to normoxic control cells (Figure 10C). While the ratio of Hsp90ab1 to β1-NKA interaction in hypoxic control cells to normoxic cells increases, this ratio decreases in hypoxic cells with silenced HIF-1α gene expression (Figure 10B,C).

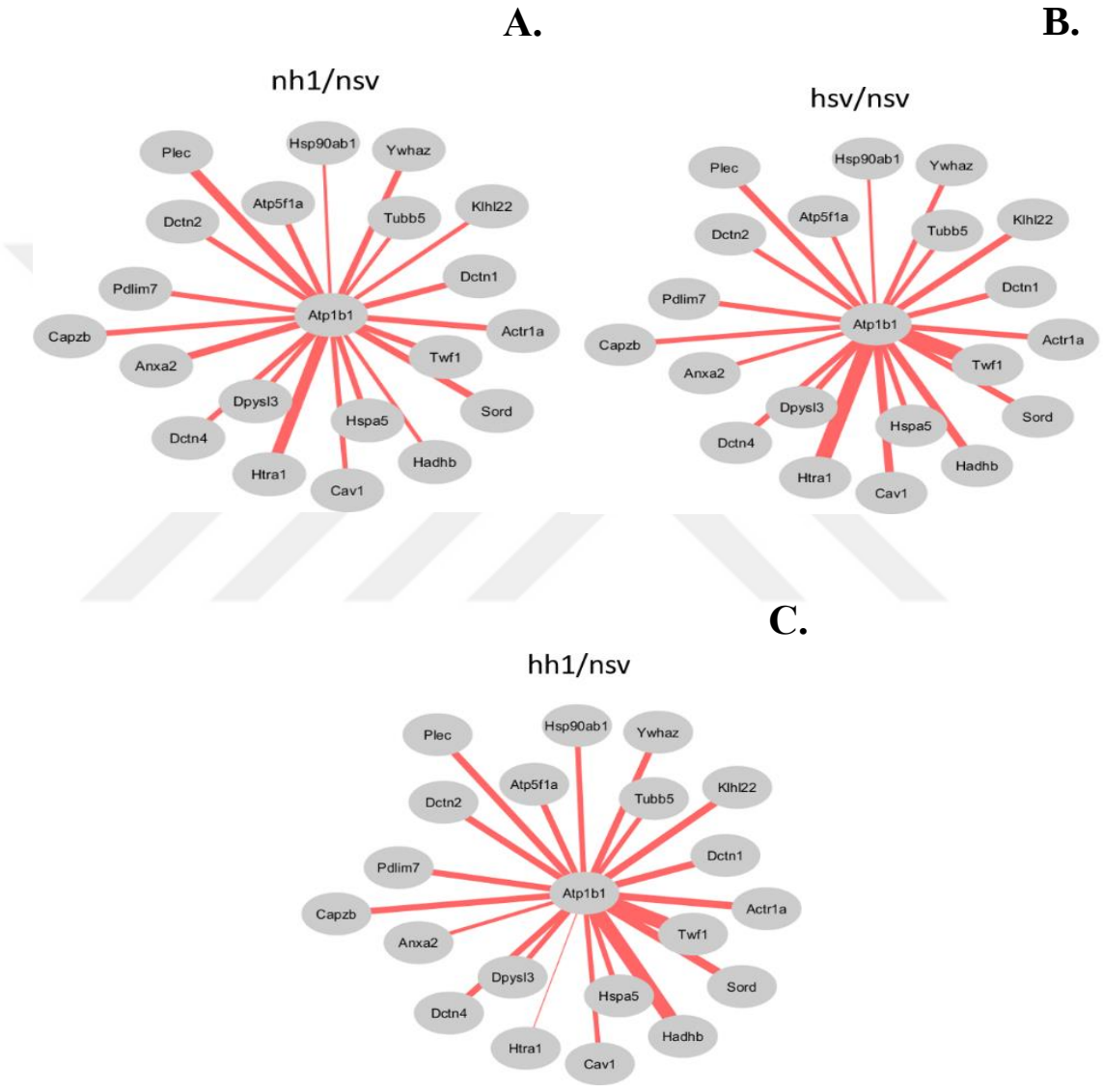

Figure 10. Visualization of protein-protein interaction network of Atp1b1 partners using Cytoscape. The thick line indicates increased protein interaction and the thin line indicates reduced interaction compared to normoxic control cells. Nsv: normoxic control cells, nh1: normoxic HIF-1α silenced cells, hsv: hypoxic control cells, hh1: hypoxic HIF-1α silenced cells.

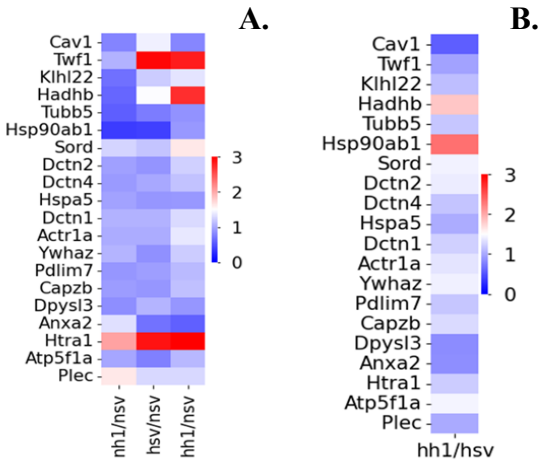

Figure 11. Color scaling of the Atp1b1 interacting common partner list according to abundace ratio of each conditions. Heat-map scaled according to nsv ratios for all three conditions (A). Heat map color scaled according to the hh1/hsv ratio (B).

Table 5: Table of abundance ratio of Atp1b1 common intreaction partners in each condition.

	nh1/nsv	hsv/nsv	hh1/nsv	hh1/hsv	n
Cav1	0.78	1.41	0.79	0.56	3
Twf1	1.04	2.96	2.83	0.96	3
Klhl22	0.66	1.21	1.35	1.12	2
Hadhb	0.6	1.49	2.72	1.83	2
Tubb5	0.55	0.74	0.86	1.16	2
Hsp90ab1	0.36	0.38	0.9	2.37	2
Sord	1.25	1.15	1.64	1.43	2
Dctn2	0.95	0.88	1.22	1.39	2
Dctn4	0.91	0.99	1.14	1.15	2
Hspa5	0.95	0.88	0.89	1.01	2
Dctn1	1.04	1.04	1.28	1.23	2
Actr1a	1.02	1.02	1.36	1.33	2
Ywhaz	1.06	0.85	1.2	1.41	2
Pdlim7	0.88	0.94	1.09	1.16	2
Capzb	0.92	0.88	1.14	1.3	2
Dpysl3	0.84	1.06	0.88	0.83	2
Anxa2	1.31	0.68	0.57	0.84	2
Htra1	2.05	2.89	3.46	1.2	2
Atp5f1a	0.98	0.76	1.08	1.42	2
Plec	1.63	1.27	1.27	1	2

4.4 Effect of Hypoxia and HIF-1α Silencing on Expression of Hsp90β in Total Cell Lysates, and Caveolin-I in the Membrane

Since we found that Hsp90β is an interacting partner of β1-NKA, we performed Western Blot experiment to examine whether its interaction is due to change in the protein levels of Hsp90β in our experimental conditions. Results showed that there is no effect of hypoxia and HIF-1α on the Hsp90β protein expression (Figure 11).

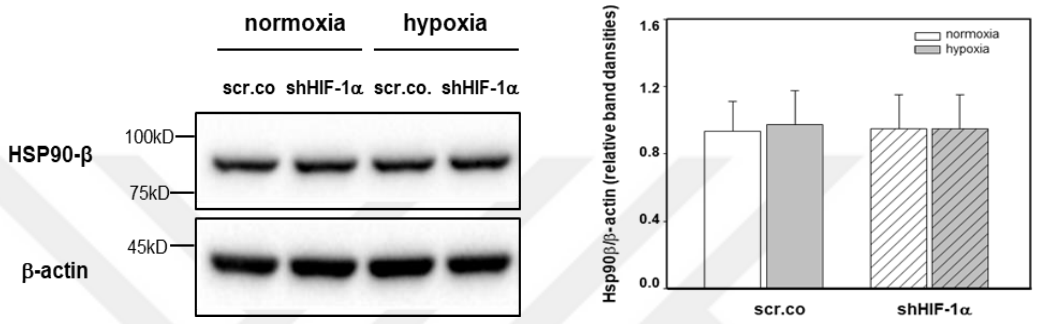

Figure 12. Effect of hypoxia and HIF-1α silencing on Hsp90β expression in whole cell lysates. Band dansities were normalized to β-actin (n=6).

Since the Caveolin-I is an integral membrane protein, its expression was investigated in the membrane fractions of H9c2 cells. Variation was observed for each condition in Western Blot experiments performed in different experimental sets. Although experimental results are highly variable, Caveolin-I expression tends to increase in hypoxia ($p > 0.05$).

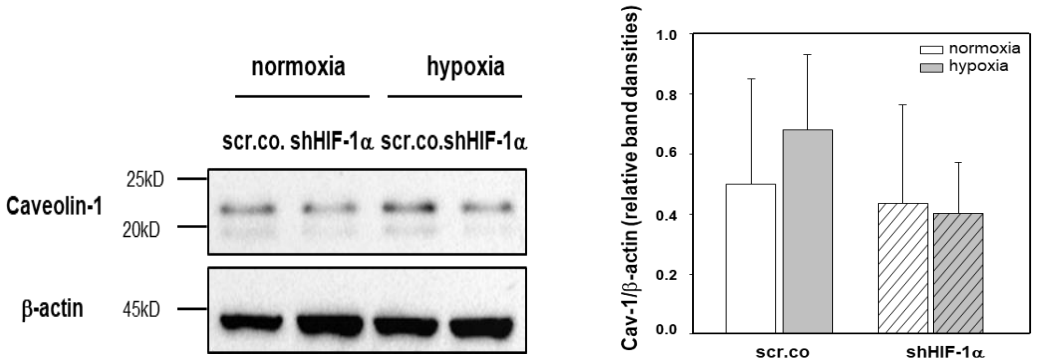

Figure 13. Effect of hypoxia and HIF-1α silencing on Caveolin-I expression in membrane preparations of H9c2 cells. Band dansities were normalized to β-actin (n=6).

4.5 Co-immunoprecipitation (Co-IP) Experiments for Confirming β1-NKA Interactions with Hsp90β and α1-NKA

In the proteomic results, we found that β1-NKA interacts with Hsp90β. It is also known that β1-NKA is required for proper localization of α1-NKA into cell membrane. To confirm Hsp90β and α1-NKA interaction with β1-NKA, co-IP was performed. Results showed that Hsp90β interacted with β1-NKA at 60kD, but not at 42kD and this interaction increased in hypoxia (Figure 13). Silencing HIF-1α in hypoxic cells decreased the interaction of Hsp90β with β1-NKA. Figure 14 shows that β1-NKA interacts with α1-NKA at around 50kD. No bands observed in positive (IgG+) and negative (IgG-) control samples.

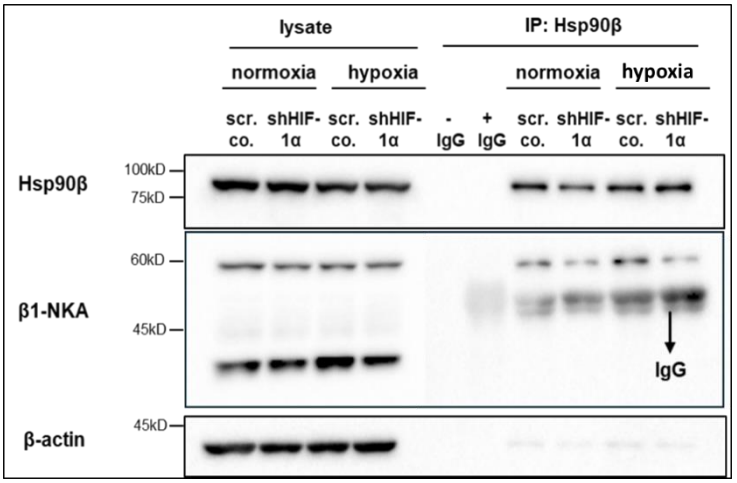

Figure 14. Co-IP experiments confirming the interaction of β1-NKA with Hsp90β. Equal amounts from whole cell lysates and elution fractions from each condition were run on gel. Positive (IgG+) and negative control (IgG-) were used.

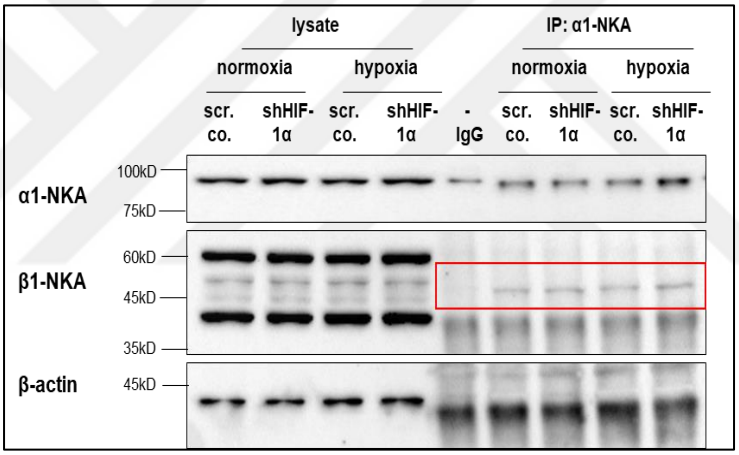

Figure 15. Co-IP experiments confirming interaction of β1-NKA with α1-NKA. Whole cell lysates and elution fractions from each condition were run on gel. Positive (IgG+) and negative control (IgG-) were used.

5 DISCUSSION

The NKA pump activity is crucial for the proper function of the heart. However, in conditions like cardiac ischemia and heart failure, NKA activity is compromised, leading to adverse effects such as Ca^{2+} overloaded, impaired diastolic function, and arrhythmias. Studies indicated decreased pump activity ~30% in tissue homogenates from different animal models of heart failure and ~ 40% in necropsy materials from human with heart failure. The reduced NKA activity has been attributed to decrease in the expression of the NKA subunits. However, the findings on isoform expression in these reports are inconsistent, and it is unknown how relative changes in the NKA subunits translate into pump activity. Moreover, most of these studies focused on the expression of α-NKA. Little is known about the expression and regulation of other subunits, which also contribute to function of the NKA. This thesis mainly focused on the regulation of β1-NKA, the subunit controls the proper membrane translocation and insertion of α-NKA, in an in-vitro ischemic heart model which is common clinical finding in CVDs and first time identified the intracellular interacting partners of β1-NKA, using proteomic and bioinformatic analysis. We also hypothesized that HIF-1α may play a role in expression and regulation of β1-NKA in hypoxic H9c2 rat ventricular cardiomyoblasts, commonly used cell line in cardiac research.

We lately reported decreased plasma membrane expression of α1- and β1-NKA in hypoxic H9c2 cells using cell surface biotinylation approach to specifically pull-down membrane proteins with streptavidin agarose beads. This study indicated that membrane expression of α1-NKA was decreased in hypoxic cells due to internalization of the proteins from plasma membrane in a HIF-1α dependent manner. On the other hand, decreased membrane expression of β1-NKA was due to internalization and degradation of the proteins, independently of HIF-1α. To identify the proteins and signaling pathways behind, we performed IP experiments using specific β1-NKA antibody and eluted the proteins interacting with β1-NKA, performed comprehensive bioinformatic analysis followed by proteomic studies. We also confirmed the identified specific interacting partners by co-IP experiments. This thesis first time reports that Caveolin-1 and Twinfilin-I are specific interacting partners of β1-NKA

and their degree of interaction is sensitive to hypoxia and HIF-1α. We also found that in hypoxic or HIF-1α silenced cells the interaction of α1-NKA and β1-NKA did not change and Hsp90β protein is another interacting protein with β1-NKA.

To identify the total expression of β1-NKA in hypoxic and HIF-1α silenced cells we performed Western Blot experiments in whole cell lysates. Results showed that β1-NKA exhibits two distinct bands at ~42kD and ~60kD. Consistent with literature, the band at ~60kD may likely be post-translational modification of the β1-NKA and the band at ~42kD is the mature form of the protein (79). The expression of β1-NKA at ~60kD remained unchanged in normoxic or hypoxic control and HIF-1α silenced cells. However, the mature form of the β1-NKA ~42kD significantly increased in hypoxic control cells compared to normoxic controls. This increase was reversed in hypoxic HIF-1α silenced cells, reaching levels comparable to normoxic cells. These findings indicate that hypoxia and HIF-1α do not affect the expression of the post-translational modification observed at 60kD. Interestingly, it increases the expression of the mature form of the protein in a HIF-1α dependent manner. This effect is not due to change in the mRNA level as we observed 15% reduction of β1-NKA in hypoxic cells (46). Considering the decreased membrane expression of β1-NKA and increased degradation shown in our previous study (46), it might be likely that membrane translocation or insertion of the mature form of the β1-NKA was blunted in hypoxic cells despite increase in the protein levels. This may also suggest that the proteins that are not translocated processed by lysosomal degradation an event to overcome the cellular stress in addition to hypoxia. For example, Vitalii et al. demonstrated that increased levels of CO2 enhance rapid ER-associated degradation of β-NKA and decrease plasma membrane abundance of the enzyme in human alveolar epithelial A549 cells and murine precision-cut lung slices (80).

Following the three repeat of successful IP experiments, LC/MS analysis were performed to identify interaction partners of β1-NKA in hypoxic and HIF-1α cells to further examine the common interaction partners that may take role in intracellular trafficking. Our results revealed in all three sets of experiments 2 proteins Caveolin-I and Twifillin-I were identified as the common interaction partners of β1-NKA. We also found that 18 common partners detected in at least two sets, and 81 proteins were

found to interact with β1-NKA exclusively in a single experiment set. The fact that only 2 proteins were identified as common partners in three independent experiments and the variation between groups may be due to standardization of proteomic experiments.

Pathway enrichment analysis using STRING and Reactome databases revealed that common interaction partners of β1-NKA are remarkably involved in pathways of immune system, cellular stress, cell division, and Golgi-ER transfer system. In 2 sets of 3 independent proteomic analysis we found that the interaction of Hsp90β protein, which is a chaperone protein. We performed co-IP experiments to confirm the interaction and found that Hsp90β - β1-NKA interaction occurs at the post-translated form of the β1-NKA and increases in hypoxic conditions which is HIF-1α dependent. Total protein expression of Hsp90β did not change in experimental conditions. Hsp90β protein may play an important role in protecting the cell's vital functions and adapting to hypoxia by stabilizing the protein folding that is disrupted under hypoxic stress. Additionally, Hsp90β has been shown to regulate cellular signaling pathways and direct the adaptation process of cells during hypoxic stress (81). The role of Hsp90β as a partner of β1-NKA needs further clarification.

Ywhaz (14-3-3 zeta/delta) proteins were determined in 2 sets of 3 independent proteomic analysis as another important interaction partners of β1-NKA. Ywhaz proteins are involved in maintaining the vital functions of the cell by taking part in signal transmission, controlling gene expression, and regulating apoptosis (82). Its abundance ratio is slightly increased in hypoxic HIF-1α silenced cells compared to hypoxic control cells. Also, important cell cycle-related proteins such as Tubb5, Dctn2, Actr1a, and Dctn1 proteins (83, 84, 85, 86) were identified as interaction partners of β1-NKA. Their abundance ratio was not significantly affected by hypoxia or HIF-1α silencing, indicating that these proteins are crucial for cell survival.

Caveolin-I (Cav-I), which was identified common in three independent experiments, is a component of the caveola structure that contributes to the function of many proteins such as G proteins, NOS, and tyrosine kinase-coupled receptors located in the cell membrane, serving as a scaffold protein (87,88). Previous studies have

shown that ouabain-mediated α1-NKA is responsible for the decrease in membrane expression through the endocytosis mechanism in renal tubule cells (89). Additionally, it has been reported that α1-NKA regulates Cav-1 expression in the cell membrane (81 90). Our data demonstrate for the first time an increase in the Cav-1 interaction with β1-NKA in hypoxic cells compared to normoxic cells. Furthermore, HIF-1α gene expression in HIF-1α silenced cells reaches levels comparable to those in normoxic cells. Therefore, Cav-1 might be responsible for endocytosis of β1-NKA that leads internalization. These findings are reported here for the first time for β1-NKA regulation. To confirm Cav-1 and β1-NKA interaction we performed co-IP experiments. However, due to low performance of the antibody we could not detect specific signal. Since the Cav-I is an integral protein, it was difficult to examine its expression in total cell lysates. Therefore, we measured the expression of Cav-1 in membrane fractions of H9c2 cells. Although results of different experimental sets were highly variable, expression of Cav-I tends to increase in hypoxic cells compared to normoxic cells.

We also found that Twifillin-I (Twf-I) is a specific interacting partner of β1-NKA. Twf-I is involved in various biological processes such as organization of the cytoskeleton, cell migration, cell adhesion, cell proliferation and survival (91). Our findings showed that the interaction of Twf-1 with β1-NKA is significantly increased in hypoxia, independent of HIF-1α. Any role of Twf-I in regulating the membrane expression of β1-NKA needs further studies.

Additionally, it has been reported that β1-NKA is responsible for the proper insertion of α1-NKA into the cell membrane (27). Here we also tested any change in α1-NKA - β1-NKA interaction in our experimental settings. Co-IP experiments showed no change in the interaction degree, indicating that despite decreased membrane expression and translocation of β1-NKA in hypoxic cells the cellular pool of β1-NKA might be still enough for maintaining the localization of α1-NKA into plasma membrane.

The aim of this thesis was to identify interaction partners of β1-NKA in hypoxic/ischemic heart model and to understand how the intracellular dynamics of the β1-NKA is regulated by hypoxia and whether HIF-1α is involved in this process. Future research, it is essential to explore the mechanisms through which these identified proteins interact and regulate the expression, consequently affecting the activity of NKA in the ischemic heart. This study has contributed new insights into the regulation of β1-NKA within the ischemic heart and defined signaling pathway in which the proteins are involved in.

6 CONCLUSIONS

This study identified interaction partners of β1-NKA in in-vitro ischemic/hypoxic heart model. It was indicated that β1-NKA interacts with proteins involved in pathways related to immune system, cellular stress, cell division, and Golgi-ER transfer system. It has been determined that the abundance ratios of specific interacting partners of Hsp90β, Cav-I and Twf-1 proteins increased in hypoxia in a HIF-1α dependent manner. Further studies are needed to explore the impact of these interactions in regulating cellular trafficking of β1-NKA in hypoxic cardiomyoblasts.

7 REFERENCES

1. Mozaffarian D, Benjamin EJ, Go AS, Arnett DK, Blaha MJ, Cushman M, et al. Heart disease and stroke statistics—2016 update: a report from the American Heart Association. circulation. 2016;133(4):e38-e360.
2. Khan MA, Hashim MJ, Mustafa H, Baniyas MY, Al Suwaidi SKBM, AlKatheeri R, et al. Global epidemiology of ischemic heart disease: results from the global burden of disease study. Cureus. 2020;12(7).
3. Moran AE, Forouzanfar MH, Roth GA, Mensah GA, Ezzati M, Murray CJ, Naghavi M. Temporal trends in ischemic heart disease mortality in 21 world regions, 1980 to 2010: the Global Burden of Disease 2010 study. Circulation. 2014;129(14):1483-92.
4. Sun B, Wang L, Guo W, Chen S, Ma Y, Wang D. New treatment methods for myocardial infarction. Frontiers in Cardiovascular Medicine. 2023;10.
5. Semenza GL. Oxygen sensing, hypoxia-inducible factors, and disease pathophysiology. Annual Review of Pathology: Mechanisms of Disease. 2014;9:47-71.
6. He J, Liu D, Zhao L, Zhou D, Rong J, Zhang L, Xia Z. Myocardial ischemia/reperfusion injury: Mechanisms of injury and implications for management. Experimental and therapeutic medicine. 2022;23(6):1-11.
7. Patel VB, Zhong J-C, Grant MB, Oudit GY. Role of the ACE2/angiotensin 1–7 axis of the renin–angiotensin system in heart failure. Circulation research. 2016;118(8):1313-26.
8. Rosano G, Fini M, Caminiti G, Barbaro G. Cardiac metabolism in myocardial ischemia. Current pharmaceutical design. 2008;14(25):2551-62.
9. Doenst T, Nguyen TD, Abel ED. Cardiac metabolism in heart failure: implications beyond ATP production. Circulation research. 2013;113(6):709-24.
10. Lopaschuk GD, Stanley WC. Glucose metabolism in the ischemic heart. Circulation. 1997;95(2):313-5.
11. Braunwald E, Mann DL, Zipes DP, Libby P, Bonow R. Braunwald's heart disease: a textbook of cardiovascular medicine. Braunwald's heart disease: A textbook of cardiovascular medicine2015. p. 1028-.
12. Wei X, Yohannan S, Richards JR. Physiology, cardiac repolarization dispersion and reserve. 2019.
13. Niggli E, Lederer WJ. Voltage-independent calcium release in heart muscle. Science. 1990;250(4980):565-8.
14. Bers DM, Barry WH, Despa S. Intracellular Na+ regulation in cardiac myocytes. Cardiovascular research. 2003;57(4):897-912.
15. Gorski PA, Ceholski DK, Hajjar RJ. Altered myocardial calcium cycling and energetics in heart failure—a rational approach for disease treatment. Cell metabolism. 2015;21(2):183-94.
16. Pivovarov AS, Calahorro F, Walker RJ. Na+/K+-pump and neurotransmitter membrane receptors. Invertebrate Neuroscience. 2019;19(1):1.

17. Rigos CF, de Lima Santos H, Yoneda JS, Montich G, Maggio B, Ciancaglini P. Cytoplasmatic domain of Na, K-ATPase α-subunit is responsible for the aggregation of the enzyme in proteoliposomes. Biophysical chemistry. 2010;146(1):36-41.
18. Felippe Gonçalves-de-Albuquerque C, Ribeiro Silva A, Ignácio da Silva C, Caire Castro-Faria-Neto H, Burth P. Na/K pump and beyond: Na/K-ATPase as a modulator of apoptosis and autophagy. Molecules. 2017;22(4):578.
19. Berry RG, Despa S, Fuller W, Bers DM, Shattock MJ. Differential distribution and regulation of mouse cardiac Na+/K+-ATPase α1 and α2 subunits in T-tubule and surface sarcolemmal membranes. Cardiovascular research. 2007;73(1):92-100.
20. Yan Y, Shapiro JI. The physiological and clinical importance of sodium potassium ATPase in cardiovascular diseases. Current opinion in pharmacology. 2016;27:43-9.
21. Jimenez T, McDermott JP, Sánchez G, Blanco G. Na, K-ATPase α4 isoform is essential for sperm fertility. Proceedings of the National Academy of Sciences. 2011;108(2):644-9.
22. Clausen MV, Hilbers F, Poulsen H. The structure and function of the Na, K-ATPase isoforms in health and disease. Frontiers in physiology. 2017;8:257141.
23. Vagin O, Sachs G, Tokhtaeva E. The roles of the Na, K-ATPase beta 1 subunit in pump sorting and epithelial integrity. Journal of bioenergetics and biomembranes. 2007;39:367-72.
24. Clifford RJ, Kaplan JH. β-Subunit overexpression alters the stoicheometry of assembled Na-K-ATPase subunits in MDCK cells. American Journal of Physiology-Renal Physiology. 2008;295(5):F1314-F23.
25. Roa-Velázquez D, Xoconostle-Cázares B, Benítez-Cardoza CG, Ortega-López J, Shoshani L, Morales-Ríos E, Gallardo-Hernández S. Expression, purification, and refolding of the recombinant extracellular domain β1-subunit of the dog Na+/K+-ATPase of the epithelial cells. Protein Expression and Purification. 2022;200:106167.
26. Clarke DN, Lowe CJ, Nelson WJ. The cadherin-catenin complex is necessary for cell adhesion and embryogenesis in Nematostella vectensis. Developmental biology. 2019;447(2):170-81.
27. Geering K. Functional roles of Na, K-ATPase subunits. Current opinion in nephrology and hypertension. 2008;17(5):526-32.
28. Blanco G, Mercer RW. Isozymes of the Na-K-ATPase: heterogeneity in structure, diversity in function. American Journal of Physiology-Renal Physiology. 1998;275(5):F633-F50.
29. McDONOUGH AA, Geering K, Farley RA. The sodium pump needs its β subunit. The FASEB journal. 1990;4(6):1598-605.
30. Vagin O, Tokhtaeva E, Sachs G. The role of the β1 subunit of the Na, K-ATPase and its glycosylation in cell-cell adhesion. Journal of biological chemistry. 2006;281(51):39573-87.
31. Silverman Bd, Fuller W, Eaton P, Deng J, Moorman JR, Cheung JY, et al. Serine 68 phosphorylation of phospholemman: acute isoform-specific activation of cardiac Na/K ATPase. Cardiovascular research. 2005;65(1):93-103.

32. Han F, Bossuyt J, Martin JL, Despa S, Bers DM. Role of phospholemman phosphorylation sites in mediating kinase-dependent regulation of the Na+-K+-ATPase. American Journal of Physiology-Cell Physiology. 2010;299(6):C1363-C9.
33. Baloglu E. Hypoxic stress-dependent regulation of Na, K-ATPase in ischemic heart disease. International Journal of Molecular Sciences. 2023;24(9):7855.
34. Shattock MJ, Ottolia M, Bers DM, Blaustein MP, Boguslavskyi A, Bossuyt J, et al. Na+/Ca2+ exchange and Na+/K+- ATPase in the heart. The Journal of physiology. 2015;593(6):1361-82.
35. Ottolia M, John S, Hazan A, Goldhaber JI. The cardiac Na+-Ca2+ exchanger: from structure to function. Comprehensive Physiology. 2021;12(1):2681.
36. Iwamoto T, Kita S, Shigekawa M. Functional analysis of Na+/Ca2+ exchanger using novel drugs and genetically engineered mice. Nihon Yakurigaku zasshi Folia Pharmacologica Japonica. 2002;120(1):91P-3P.
37. Despa S, Bers DM. Na+ transport in the normal and failing heart—remember the balance. Journal of molecular and cellular cardiology. 2013;61:2-10.
38. Bogdanova A, Ogunshola OO, Bauer C, Nikinmaa M, Gassmann M. Molecular mechanisms of oxygen-induced regulation of Na+/K+ pump. Chemoreception: From Cellular Signaling to Functional Plasticity: Springer; 2003. p. 231-8.
39. Pike MM, Luo CS, Clark MD, Kirk KA, Kitakaze M, Madden MC, et al. NMR measurements of Na+ and cellular energy in ischemic rat heart: role of Na (+)-H+ exchange. American Journal of Physiology-Heart and Circulatory Physiology. 1993;265(6):H2017-H26.
40. Schwinger RH, Wang J, Frank K, Müller-Ehmsen J, Brixius K, McDonough AA, Erdmann E. Reduced sodium pump α1, α3, and β1-isoform protein levels and Na+, K+-ATPase activity but unchanged Na+-Ca2+ exchanger protein levels in human heart failure. Circulation. 1999;99(16):2105-12.
41. Semb SO, Lunde PK, Holt E, Tønnessen T, Christensen G, Sejersted OM. Reduced myocardial Na+, K+-pump capacity in congestive heart failure following myocardial infarction in rats. Journal of molecular and cellular cardiology. 1998;30(7):1311-28.
42. Aksentijević D, Shattock MJ. With a grain of salt: Sodium elevation and metabolic remodelling in heart failure. Journal of molecular and cellular cardiology. 2021;161:106-15.
43. Despa S, Islam MA, Pogwizd SM, Bers DM. Intracellular [Na+] and Na+ pump rate in rat and rabbit ventricular myocytes. The Journal of physiology. 2002;539(1):133-43.
44. Pogwizd SM, Sipido KR, Verdonck F, Bers DM. Intracellular Na in animal models of hypertrophy and heart failure: contractile function and arrhythmogenesis. Cardiovascular research. 2003;57(4):887-96.
45. Loeh B, Baloglu E, Ke A, Bärtsch P, Mairbäurl H. β 2-adrenergic stimulation blunts inhibition of epithelial ion transport by hypoxia of rat alveolar epithelial cells. Cellular Physiology and Biochemistry. 2009;25(1):123-34.

46. Gurler B, Gencay G, Baloglu E. Hypoxia and HIF-1α Regulate the Activity and Expression of Na, K-ATPase Subunits in H9c2 Cardiomyoblasts. Current Issues in Molecular Biology. 2023;45(10):8277-88.
47. Verdonck F, Volders PG, Vos MA, Sipido KR. Intracellular Na+ and altered Na+ transport mechanisms in cardiac hypertrophy and failure. Journal of molecular and cellular cardiology. 2003;35(1):5-25.
48. Swift F, Birkeland JAK, Tovsrud N, Enger UH, Aronsen JM, Louch WE, et al. Altered Na+/Ca2+-exchanger activity due to downregulation of Na+/K+-ATPase α2-isoform in heart failure. Cardiovascular research. 2008;78(1):71-8.
49. Nakane M. Biological effects of the oxygen molecule in critically ill patients. Journal of Intensive Care. 2020;8(1):95.
50. Davis CK, Jain SA, Bae O-N, Majid A, Rajanikant G. Hypoxia mimetic agents for ischemic stroke. Frontiers in cell and developmental biology. 2019;6:175.
51. Semenza GL. Vascular responses to hypoxia and ischemia. Arteriosclerosis, thrombosis, and vascular biology. 2010;30(4):648-52.
52. Metzen E, Wolff M, Fandrey J, Jelkmann W. Pericellular PO2 and O2 consumption in monolayer cell cultures. Respiration physiology. 1995;100(2):101-6.
53. McGettrick AF, O'Neill LA. The role of HIF in immunity and inflammation. Cell metabolism. 2020;32(4):524-36.
54. Beaudry M, Hidalgo M, Launay T, Bello V, Darribère T. Regulation of myogenesis by environmental hypoxia. Journal of cell science. 2016;129(15):2887-96.
55. Sleiman SF, Speer RE, Karuppagounder SS, Basso M, Kumar A, Brand D, et al. Hypoxia-inducible factor prolyl hydroxylases as targets for neuroprotection by "antioxidant" metal chelators. 2013.
56. Hu C-J, Sataur A, Wang L, Chen H, Simon MC. The N-terminal transactivation domain confers target gene specificity of hypoxia-inducible factors HIF-1α and HIF-2α. Molecular biology of the cell. 2007;18(11):4528-42.
57. Semenza GL. Hypoxia-inducible factors in physiology and medicine. Cell. 2012;148(3):399-408.
58. Maxwell PH, Wiesener MS, Chang G-W, Clifford SC, Vaux EC, Cockman ME, et al. The tumour suppressor protein VHL targets hypoxia-inducible factors for oxygen-dependent proteolysis. Nature. 1999;399(6733):271-5.
59. Huang LE, Gu J, Schau M, Bunn HF. Regulation of hypoxia-inducible factor 1α is mediated by an O2-dependent degradation domain via the ubiquitin-proteasome pathway. Proceedings of the National Academy of Sciences. 1998;95(14):7987-92.
60. Liu M, Galli G, Wang Y, Fan Q, Wang Z, Wang X, Xiao W. Novel therapeutic targets for hypoxia-related cardiovascular diseases: the role of HIF-1. Frontiers in physiology. 2020;11:774.
61. Semenza GL. Hypoxia-inducible factor 1 and cardiovascular disease. Annual review of physiology. 2014;76:39-56.

62. Patterson AJ, Xiao D, Xiong F, Dixon B, Zhang L. Hypoxia-derived oxidative stress mediates epigenetic repression of PKCε gene in foetal rat hearts. Cardiovascular research. 2012;93(2):302-10.
63. Lopaschuk GD, Jaswal JS. Energy metabolic phenotype of the cardiomyocyte during development, differentiation, and postnatal maturation. Journal of cardiovascular pharmacology. 2010;56(2):130-40.
64. Sack MN, Rader TA, Park S, Bastin J, McCune SA, Kelly DP. Fatty acid oxidation enzyme gene expression is downregulated in the failing heart. Circulation. 1996;94(11):2837-42.
65. Razeghi P, Young ME, Alcorn JL, Moravec CS, Frazier O, Taegtmeyer H. Metabolic gene expression in fetal and failing human heart. Circulation. 2001;104(24):2923-31.
66. Krishnan J, Suter M, Windak R, Krebs T, Felley A, Montessuit C, et al. Activation of a HIF1α-PPARγ axis underlies the integration of glycolytic and lipid anabolic pathways in pathologic cardiac hypertrophy. Cell metabolism. 2009;9(6):512-24.
67. el Alaoui-Talibi Z, Landormy S, Loireau A, Moravec J. Fatty acid oxidation and mechanical performance of volume-overloaded rat hearts. American Journal of Physiology-Heart and Circulatory Physiology. 1992;262(4):H1068-H74.
68. Sato T, Takeda N. The roles of HIF-1α signaling in cardiovascular diseases. Journal of cardiology. 2023;81(2):202-8.
69. Sui X, Wei H, Wang D. Novel mechanism of cardiac protection by valsartan: synergetic roles of TGF- β1 and HIF- 1α in Ang II- mediated fibrosis after myocardial infarction. Journal of cellular and molecular medicine. 2015;19(8):1773-82.
70. Su F, Zhang W, Chen Y, Ma L, Zhang H, Wang F. Significance of hypoxia-inducible factor‐1α expression with atrial fibrosis in rats induced with isoproterenol. Experimental and Therapeutic Medicine. 2014;8(6):1677-82.
71. Baloglu E, Nonnenmacher G, Seleninova A, Berg L, Velineni K, Ermis-Kaya E, Mairbäurl H. The role of hypoxia-induced modulation of alveolar epithelial Na+-transport in hypoxemia at high altitude. Pulmonary Circulation. 2020;10(1_suppl):50-8.
72. Xu Q, Arevalo MT, Pichichero ME, Zeng M. A new complementing cell line for replication-incompetent E1–deleted adenovirus propagation. Cytotechnology. 2006;51:133-40.
73. Joshi-Tope G, Gillespie M, Vastrik I, D'Eustachio P, Schmidt E, de Bono B, et al. Reactome: a knowledgebase of biological pathways. Nucleic acids research. 2005;33(suppl_1):D428-D32.
74. Mering Cv, Huynen M, Jaeggi D, Schmidt S, Bork P, Snel B. STRING: a database of predicted functional associations between proteins. Nucleic acids research. 2003;31(1):258-61.
75. Szklarczyk D, Kirsch R, Koutrouli M, Nastou K, Mehryary F, Hachilif R, et al. The STRING database in 2023: protein–protein association networks and functional enrichment analyses for any sequenced genome of interest. Nucleic acids research. 2023;51(D1):D638-D46.
76. Killcoyne S, Carter GW, Smith J, Boyle J. Cytoscape: a community-based framework for network modeling. Protein networks and pathway analysis. 2009:219-39.

77. Smoot ME, Ono K, Ruscheinski J, Wang P-L, Ideker T. Cytoscape 2.8: new features for data integration and network visualization. Bioinformatics. 2011;27(3):431-2.
78. Doncheva NT, Morris JH, Holze H, Kirsch R, Nastou KC, Cuesta-Astroz Y, et al. Cytoscape stringApp 2.0: analysis and visualization of heterogeneous biological networks. Journal of proteome.
79. Ding B, Walton JP, Zhu X, Frisina RD. Age-related changes in Na, K-ATPase expression, subunit isoform selection and assembly in the stria vascularis lateral wall of mouse cochlea. Hearing Research. 2018;367:59-73.
80. Kryvenko V, Vadász I. Novel transfection methods in primary lung cell cultures. American Journal of Physiology-Lung Cellular and Molecular Physiology. 2021.
81. Xiong L, Zhao T, Huang X, Liu Z-h, Zhao H, Li M-m, et al. Heat shock protein 90 is involved in regulation of hypoxia-driven proliferation of embryonic neural stem/progenitor cells. Cell Stress and Chaperones. 2009;14(2):183-92.
82. Gardino AK, Yaffe MB, editors. 14-3-3 proteins as signaling integration points for cell cycle control and apoptosis. Seminars in cell & developmental biology; 2011: Elsevier.
83. Breuss M, Fritz T, Gstrein T, Chan K, Ushakova L, Yu N, et al. Mutations in the murine homologue of TUBB5 cause microcephaly by perturbing cell cycle progression and inducing p53-associated apoptosis. Development. 2016;143(7):1126-33.
84. Li W, Chen J, Xiong Z, Zhou H, Huang S, Ren J, et al. Dynactin 2 acts as an oncogene in hepatocellular carcinoma through promoting cell cycle progression. Liver Research. 2022;6(3):155-66.
85. Mostafa Kamal AH, Aloor JJ, Fessler MB, Chowdhury SM. Crosslinking Proteomics Indicates Effects of Simvastatin on the TLR2 interactome and Reveals ACTR1A as a Novel Regulator of the TLR2 Signal Cascade. bioRxiv. 2019:530402.
86. Chen TY, Syu JS, Han TY, Cheng Hl, Lu FI, Wang CY. Cell Cycle- Dependent Localization of Dynactin Subunit p150glued at Centrosome. Journal of Cellular Biochemistry. 2015;116(9):2049-60.
87. Zundel W, Swiersz LM, Giaccia A. Caveolin 1-mediated regulation of receptor tyrosine kinase-associated phosphatidylinositol 3-kinase activity by ceramide. Molecular and cellular biology. 2000;20(5):1507-14.
88. Parat M-O, Riggins GJ. Caveolin-1, caveolae, and glioblastoma. Neuro-oncology. 2012;14(6):679-88.
89. Liu J. Ouabain-induced endocytosis and signal transduction of the Na/K-ATPase. Front Biosci. 2005;10(2056-2063):15970478.
90. Cai T, Wang H, Chen Y, Liu L, Gunning WT, Quintas LEM, Xie Z-J. Regulation of caveolin-1 membrane trafficking by the Na/K-ATPase. The Journal of cell biology. 2008;182(6):1153-69.
91. Li, Y., Wang, D., Ge, H., Güngör, C., Gong, X., & Chen, Y. (2022). Cytoskeletal and cytoskeleton-associated proteins: key regulators of cancer stem cell properties. Pharmaceuticals, 15(11), 1369.

8 CURRICULUM VITAE